DOE/SF/71007--T6

Program: Fuel-Transfer Machine-Component Test	MASTER
AEC Task: 7 — Fuel-Transfer Machine-Component Test	
Program Manager: G. W. Meyers	Project Manager: K. W. Foster
Reporting Period: GFY 1974	Category: HN 01 01 01.3
General Order: 09002	Subaccount: 41111, 41291, 41391 189a Number: 13638

Principal Investigators: L. G. Kellogg, E. Moody, C. E. Jones

AT03-76SF71007

DOE/SF/71007--T6

DE82 011088

I. PROJECT OBJECTIVES

The objectives of this program are to conduct the development and testing necessary to produce reliable and adequate handling devices for core components for an LMFBR plant utilizing under-the-shield refueling and reactor vessel cover rotating plugs. Component performance in the following three specific areas of concern will be investigated: (1) a reliable rising stem, vertical motion, in-vessel transfer machine (IVTM) for use in an under-the-shield refueling system with multiple rotating reactor vessel covers, (2) an ex-vessel transfer machine (EVTM) for off-line removal of fuel from the reactor in-vessel storage, and (3) ancillary fuel handling equipment, such as auxiliary handling machines (AHM), floor valves, and core component service equipment.

II. TECHNICAL PROGRESS DURING FISCAL YEAR 1974

A. SUMMARY

Two major testing programs were conducted during the fiscal year — the IVTM Seal and Bushing Test, and the EVTM Parametric Heat Transfer Test. The former test was completed through Phase III, which covered normal IVTM operation, showing the seal and bushing design to be quite adequate. The latter test was completed successfully, resulting in attainment of important knowledge of the sodium natural convection patterns which develop in a fuel assembly immersed in sodium in a canister (CCP). The Phase IV IVTM test, to determine temperature limits of the seals, was initiated at the end of the year.

7-12-74

DISCLAIMER

DOE/SF/71007--T6

The Task 7 Program Plan was redefined (PP-099-411-001) to account for work scope and CRBRP design and refueling concept changes which have occurred since the inception of the Task. Figures 1 through 3 show the testing schedules for the major subtasks (i.e., A — IVTM, B — EVTM, and C — Ancillary Equipment.

Initiation of all remaining EVTM testing was accomplished. A full-scale cold wall test is in the fabrication stage at HEDL. This test is a combination EVTM-CLEM test, wherein AI has the responsibility for defining test requirements and insuring that the test is designed and run to attain required goals, while HEDL has the responsibility for designing, fabricating, and conducting the test. The remaining tests, two to determine effective EVTM emissivities, one to verify operation of a CCP siphon to reduce drip pan loading and improve heat transfer, and one to determine the effects of operating the grapple suspension member in sodium, are in the design phase at AI. Partial material acquisition has been made, and fabrication will begin in the first month of GFY 1975.

Trade studies were conducted, with the goal of simplifying the refueling system and reducing Reactor Containment Building (RCB) size. These studies identified a new test requirement for sodium-immersed chains used for a shortened EVTM. The short EVTM concept has been adopted as the reference EVTM design. The reduced height is required for passage through the containment hatch between the RCB and Reactor Services Building (RSB).

B. DISCUSSION

Task 7 is subdivided into four major subtasks, as follows:

Subtask A — In-Vessel Transfer Machine (IVTM)
Subtask B — Ex-Vessel Transfer Machine (EVTM)
Subtask C — Ancillary Equipment
Subtask D — Engineering Studies

The technical progress attained in each of these subtasks is described in the following sections.

1. Subtask A — In-Vessel Transfer Machine (IVTM)

Four tests are planned for this machine. Only one, the seal and bushing test, has been implemented to date. Requests for test for the other three have been released, as follows:

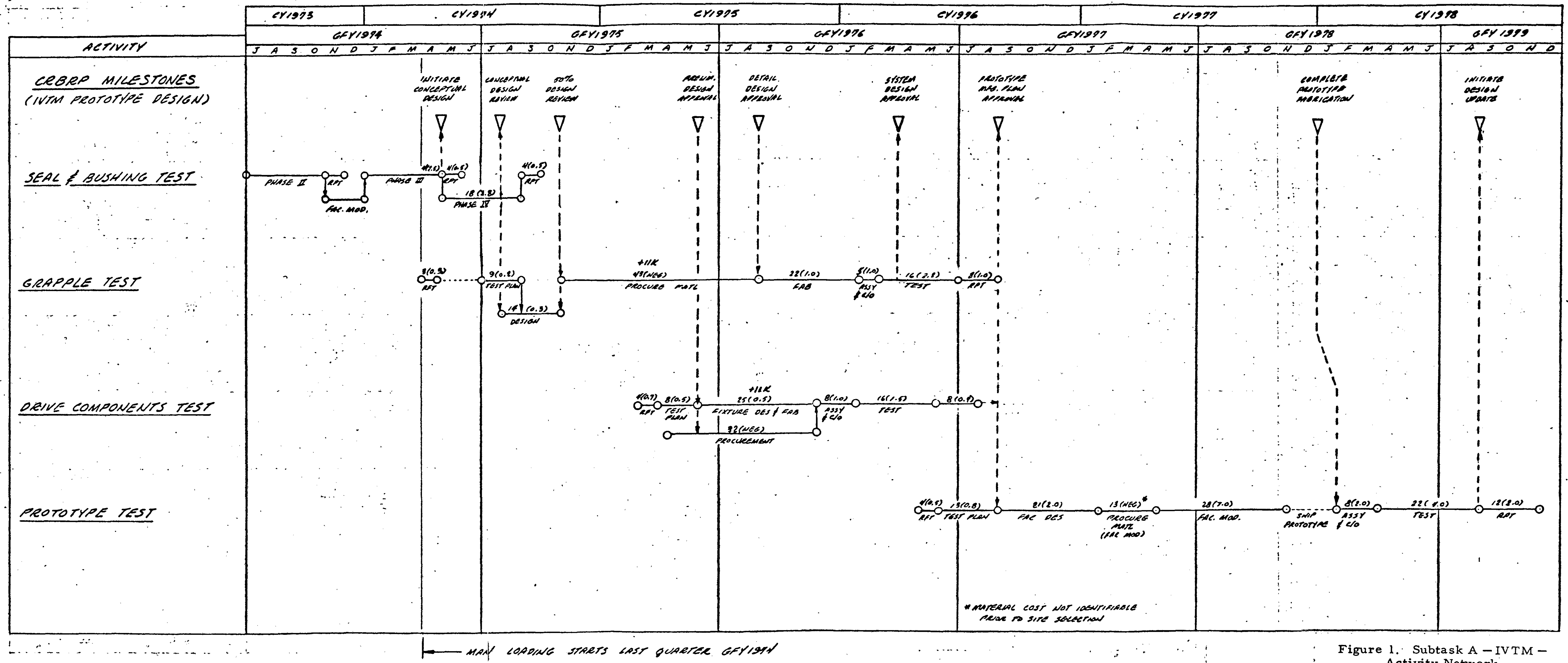

Figure 1. Subtask A – IVTM – Activity Network

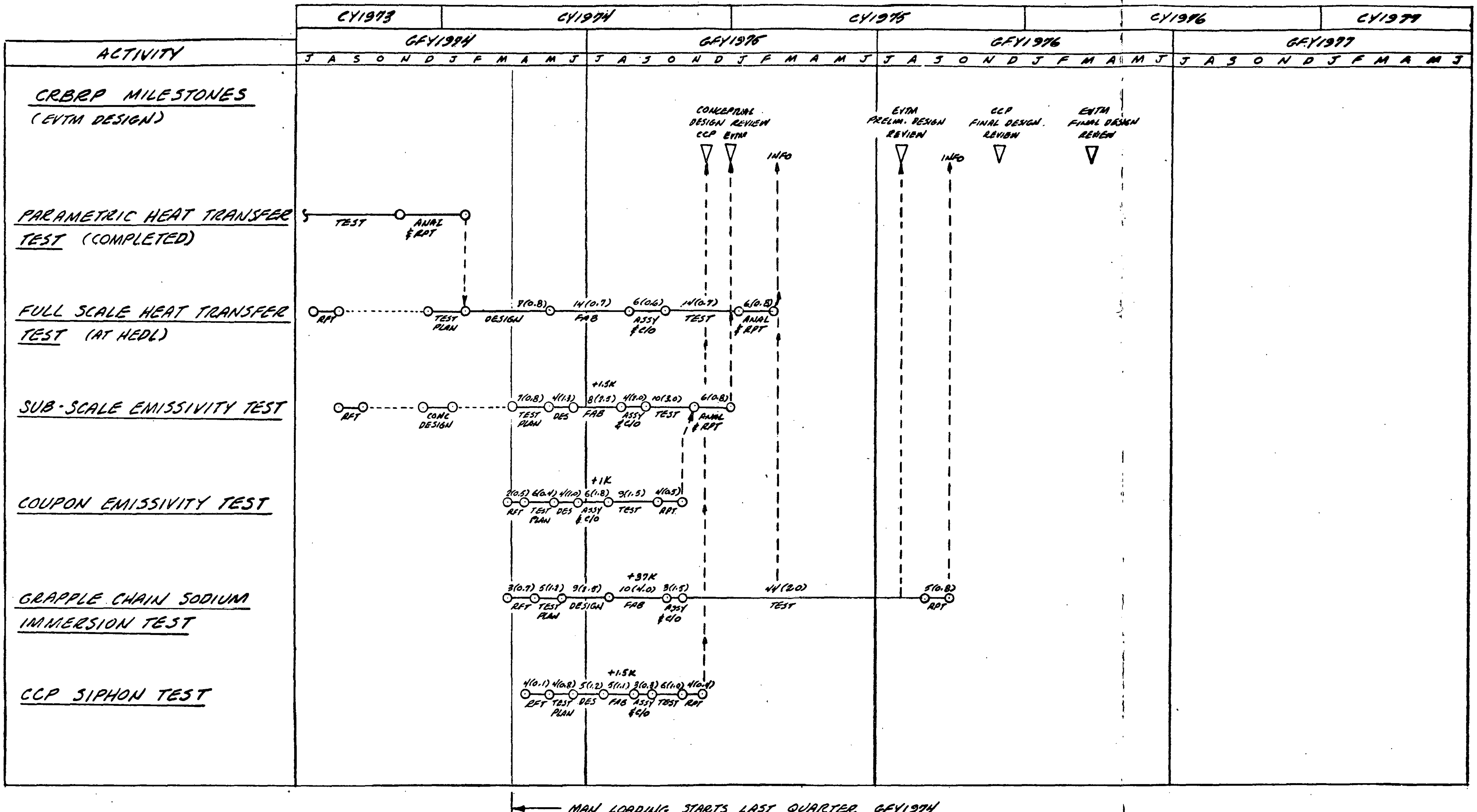

Figure 2. Subtask B – EVTM – Activity Network

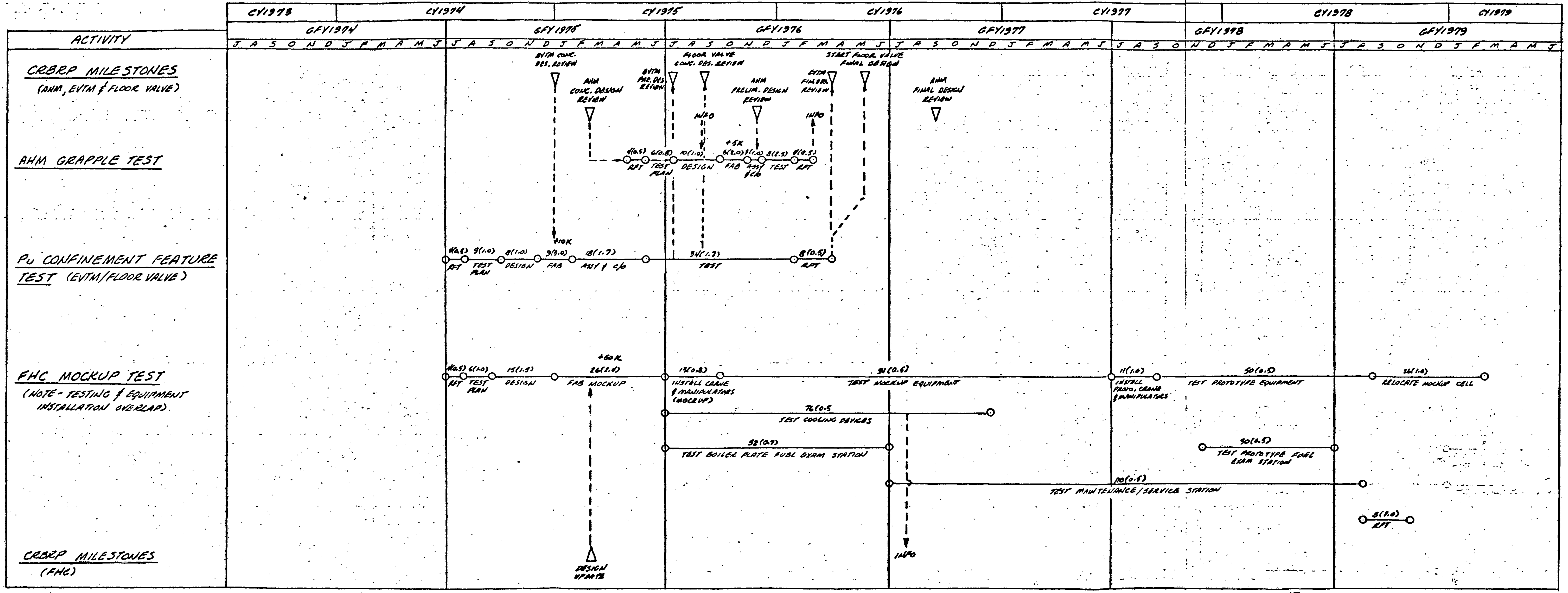

Figure 3. Subtask C — Ancillary Equipment — Activity Network

RFT-099-412-002 (DAD 41.1.03) — IVTM Drive Components Test

RFT-099-412-003 (DAD 41.1.02) — IVTM Grapple Misalignment Test

RFT-099-412-004 (DAD 41.1.04) — IVTM Prototype Test

a. Seal and Bushing Test

Phase II testing (first seal and bushing test, tested under reactor refueling conditions) of proposed seals, wipers, and guide bushings for the rising stem IVTM was completed in June 1973. Post-test examination of the test articles was completed early during this fiscal year. The test articles (see Table 1) were the seals and bushings recommended from previously conducted Phase I ambient scoping tests.*

Testing was conducted over a 500°F sodium pool for 102 days (real time). The simulated IVTM rising stem was automatically cycled to simulate actual fuel transfer machine dynamics — specifically, stem travel and speed (linear and rotational) and maximum time in the up position (which imposes a maximum time at temperature condition upon the seals). Simulated and actual IVTM transfer cycles are shown in Figure 4. Minimum and desired design goals for the test articles are shown in Table 2. The actual total feet of linear travel for the test system was 311,000 ft, equivalent to 7 years of operation. Seal and upper nylon bushing performance was found to be satisfactory, with no measurable wear or degradation. The lower Stellite guide bushing was found to have machined grooves, ~1 to 2 mils deep, along the length of the rod, and new bushing designs are now being considered. For this application (see Figures 5 and 6), elastomer rod wipers used in the seal housing performed satisfactorily, in that they showed little or no sign of wear, but there was reason to believe that they may have been a contributing cause to migration of seal lubricant and of the seal housing. Design modifications were undertaken to correct this deficiency (see Figure 7).

The seals and wipers tested were lubricated with what was considered an absolute minimum amount of silicone grease, Dow-55M. The lubricant was fed through a plenum above the seals with the aid of a spring-loaded grease cup.

*TR-097-241-001, "Test Report (Development) — FTM Stem Seals and Bushings, Phase I, Ambient Scoping Tests," January 5, 1973.

TABLE 1

PHASE II TEST ARTICLES

1.	Four T-Ring seals, Greene Tweed Company Part No. 7345FT-952-N, Ethylene Propylene, plus associated nylon backup rings (Spec. L-P4-10a)
2.	Two rod wipers, Parker Seal Company Part No. 8600-0400, Compound E540-8
3.	Two nylon bushings

TABLE 2

IVTM DUTY CYCLES

Operating Life	IVTM Design Requirements	Seal and Bushing Test Article Requirements
1-year Operation		
Number of cycles*	392†	366
Linear feet of travel* through the seal	43,920 ft†	43,920 ft
Number of grapple stem rotations	392 (180°F)	500 (225°F)
5-year Operation		
Number of cycles	1960	1830
Linear feet of travel through the seals	219,600 ft	219,600 ft
Number of grapple stem rotations	1960 (180°F)	1560 (225°)

*See Figure 4 for definition of travel.
†Two refueling periods per year.

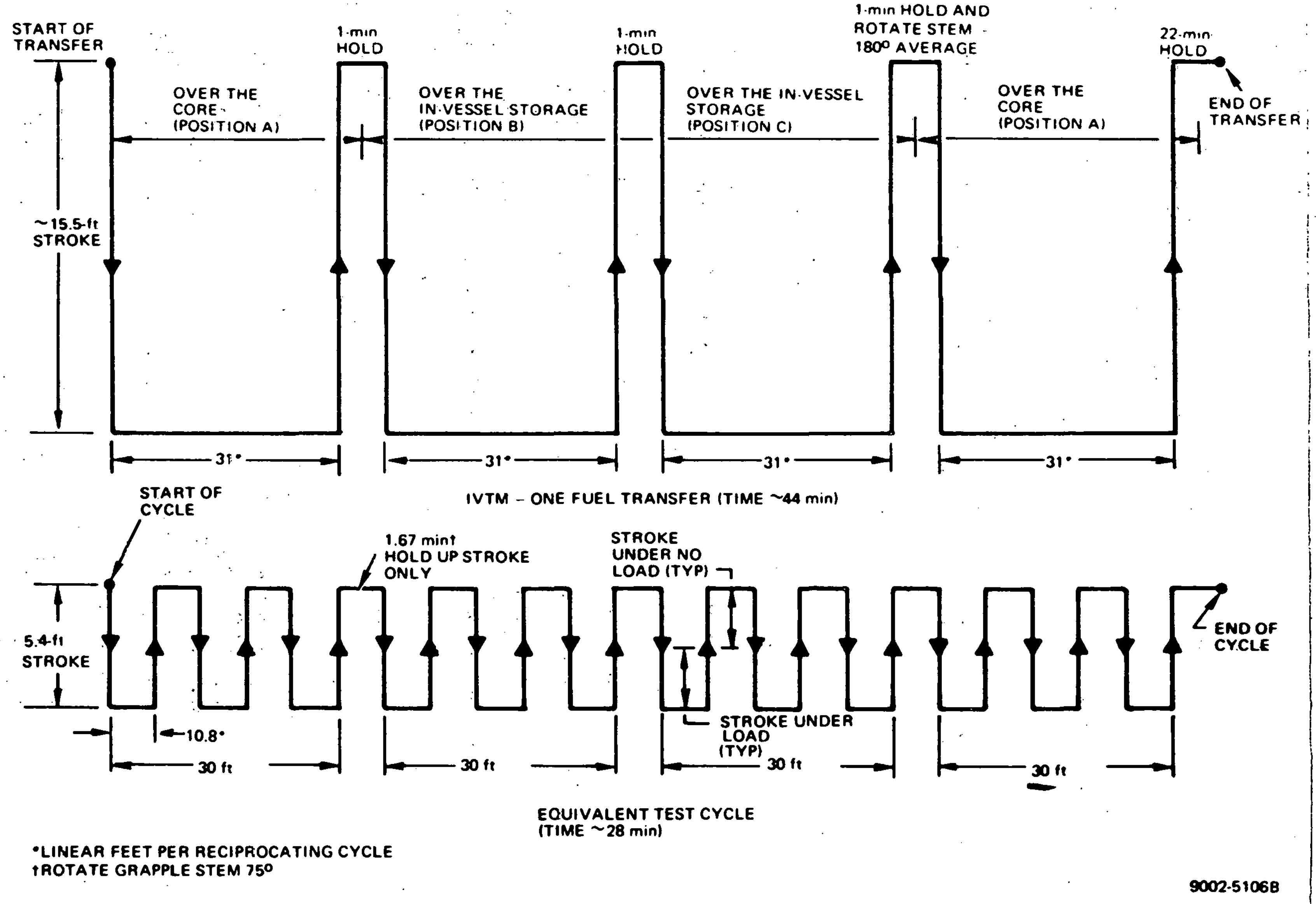

Figure 4. Seal and Bushing Test Cycle Definition

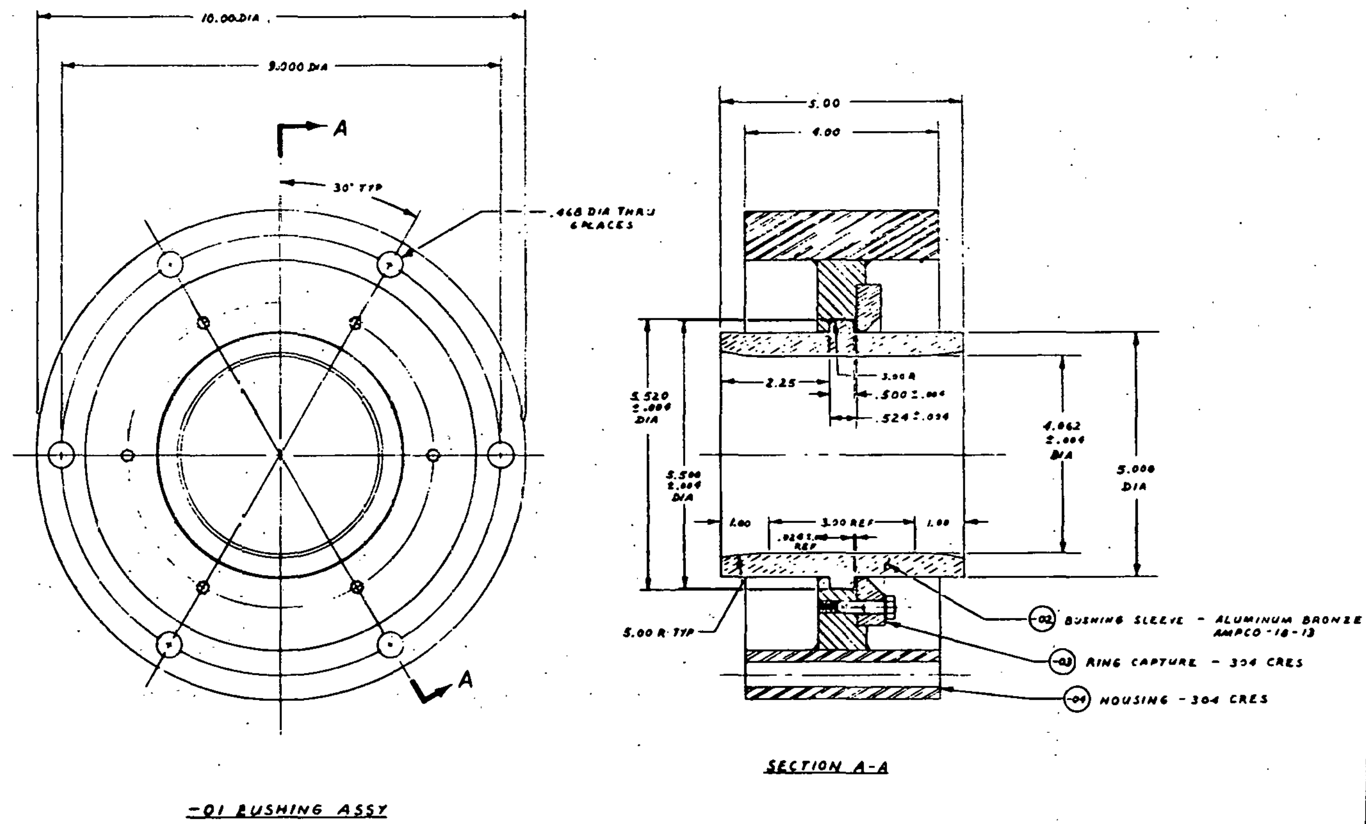

Figure 5. Bushing Guide Assembly (Dwg EX-N097241056)

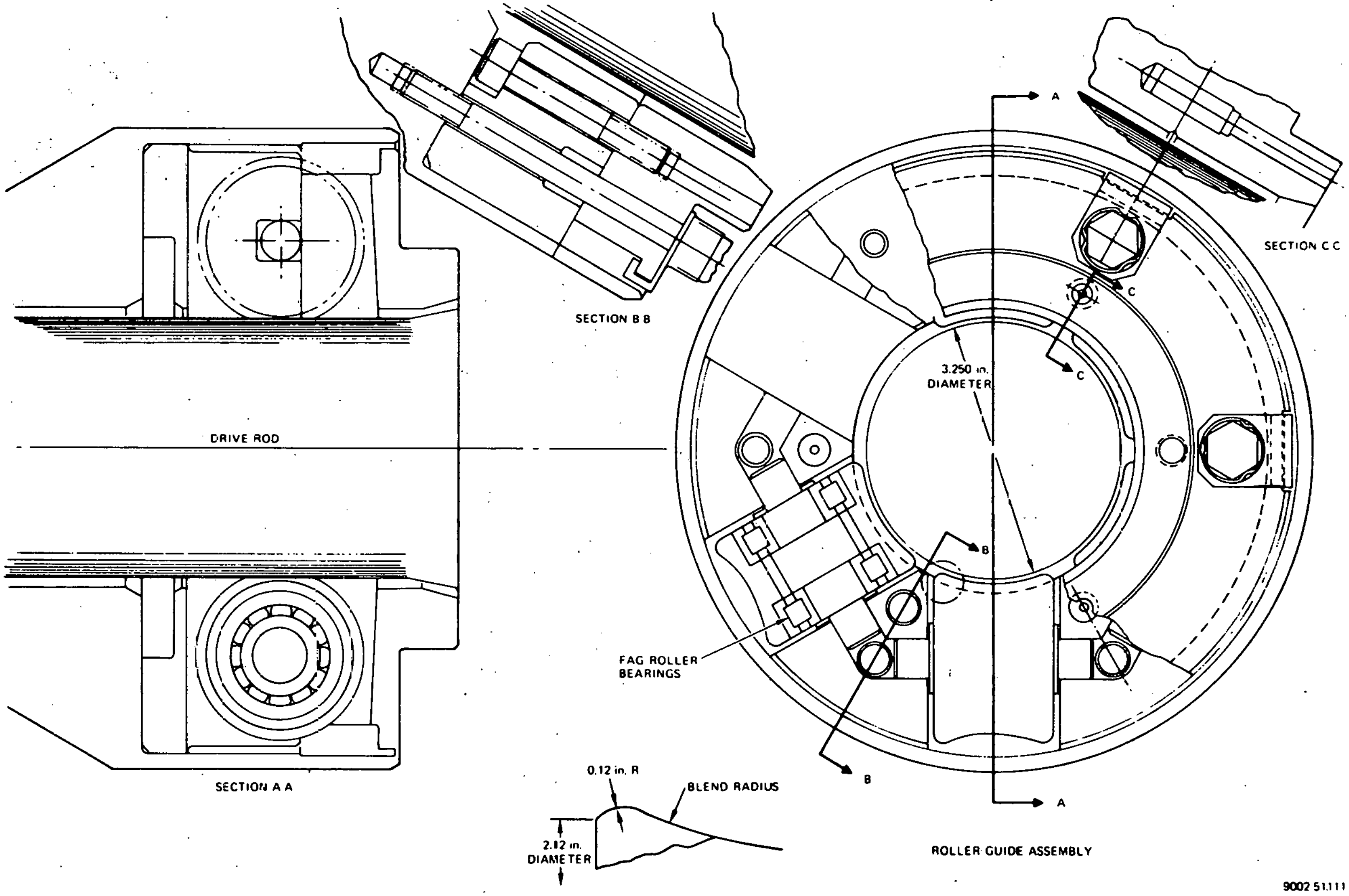

Figure 6. Roller Guide Assembly

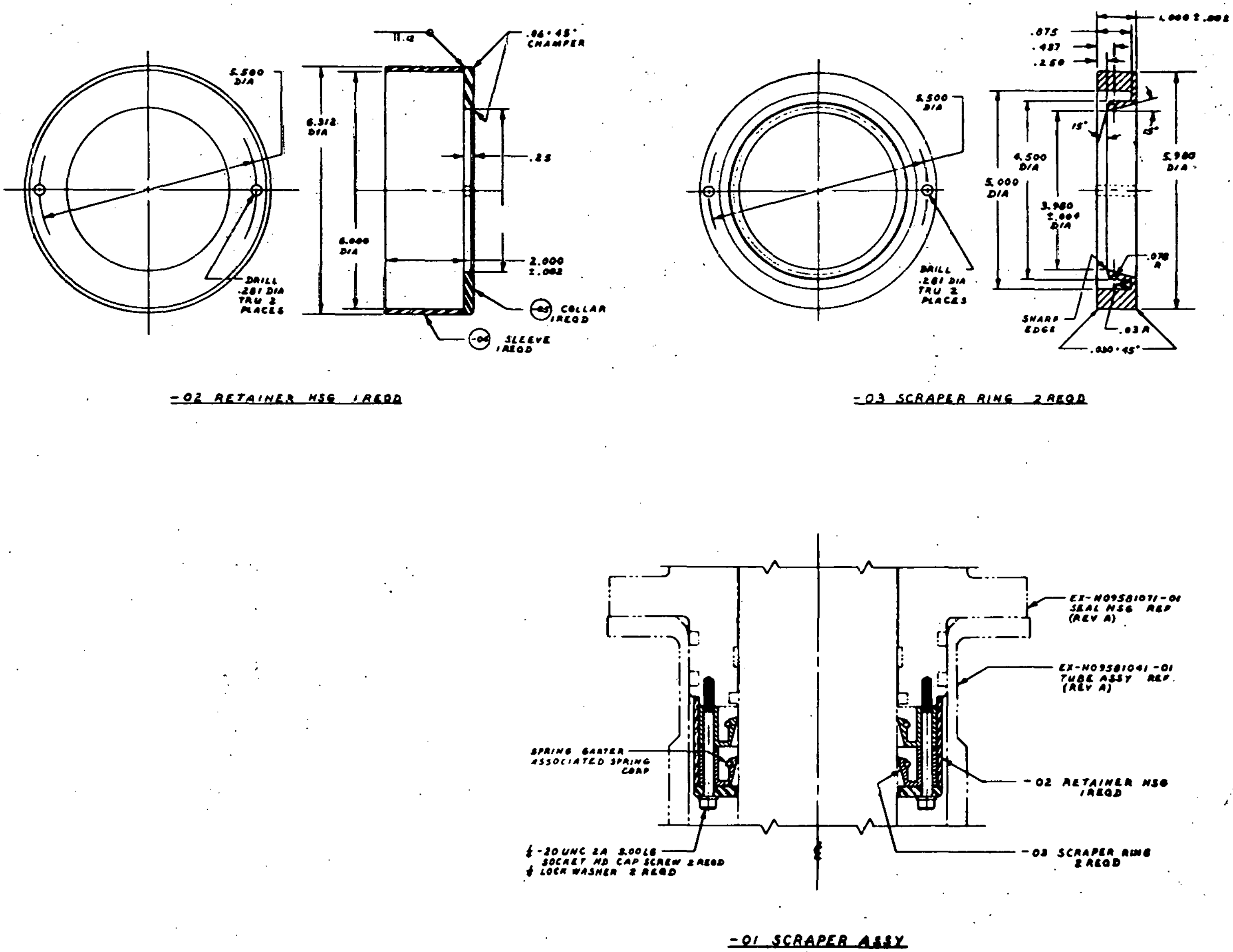

Figure 7. Scraper Assembly (Dwg EX-N097241059)

Lubricant addition or consumption was ~0.19 to 0.24 mg/ft of stem travel, and was constant during the course of the test. Addition of lubricant was based on the onset of rapidly increasing seal drag (e.g., lubricant was added to the grease cup only when a sharp increase in drag was noted). A total of 58.9 gm of lubricant was used during the test. The disposition of the lubricant at the end of testing was found to be as follows:

	gm
Lubricant accumulated above housing	12.5
Lubricant remaining on seals	5.6
Lubricant remaining in housing	4.5
Lubricant removed from stem rod	1.9
Lubricant removed from ledge below housing	3.6
Lubricant removed from sleeve around stem	2.0
Lubricant washed from sodium tank	11.1
Total	41.2

This accounts for ~69% of the total Dow-55M consumed. At the most, 28.8 gm of lubricant were transferred to the sodium tank during the 7 years of simulated reactor operation. Sodium in the tank had a final carbon content of 4 ppm, corresponding to the solution of ~0.1 gm of carbon, presumably from the 28.8 gm of lubricant that may have been transferred into the tank.

During the latter portion of the test, the lubricant was found to have degraded to a black, waxy texture which tended to gum up into balls and flakes. The same degradation had also been noted in other high-temperature seal tests at AI, which were not exposed to sodium. The degradation is thus believed to be strictly thermal degradation, and not due to any chemical action resulting from the sodium environment. Figure 8 shows the fresh Dow-55M, and as removed from the seal housing at the end of testing. It is felt that, if a sufficient quantity of this material were allowed to collect, seal performance would be impaired.

The rod wipers used on this test were designed for industrial use, and their main purpose is to keep foreign material that might damage the seals out of the seal housing. Their design then can be said to be biased in direction —

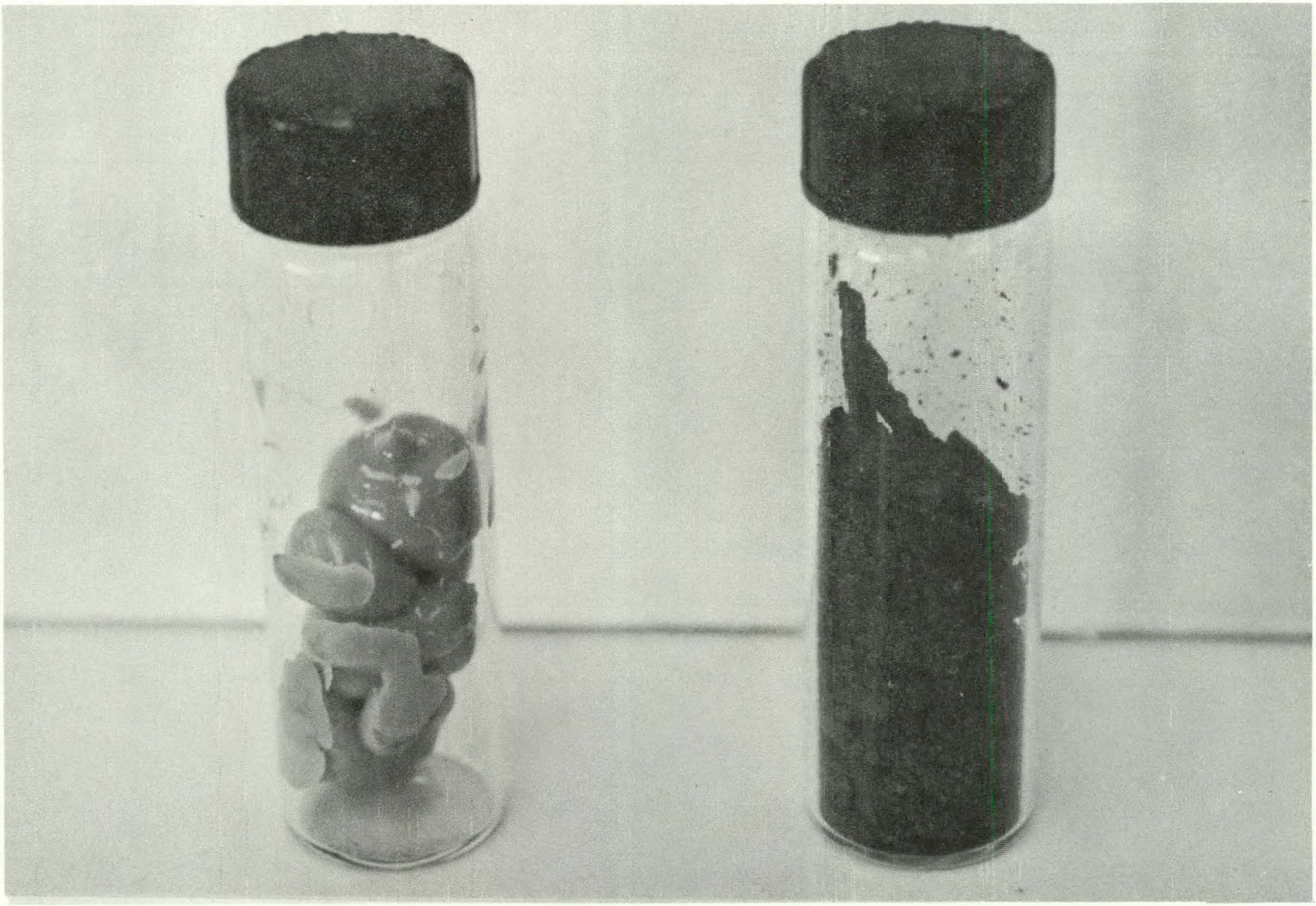

9002-4053CN

Figure 8. Dow-55M Lubricant Before and After Test

wiping material from the rod as it is stroked into the housing, and allowing some material (e.g., lubricant) to bypass it as the rod is stroked out of the housing. This one-way valving action essentially created a lubricant pump. The measured consumption rate of lubricant during the test corresponded to the wiping of a layer of lubricant only 19 to 24 Å (approximately a monomolecular layer) thick from the rod with each stroke. On the upstroke, this material collected on the outer edge of the wiper and was sloughed off (and hence contaminated the sodium tank) as it built up. Some of this material was left on the rod as a lubricant "terminal moraine" at the upper and lower extremes of the stroke.

As a secondary test objective, sodium deposition measurements were made along the stem rod and the inner diameter of the rod guide sleeve. These measurements are required to provide data needed for calculating the required amount of radiological shielding on the IVTM. The distribution found at the end of testing is shown in Figure 9.

The test report, TR-097-241-002, on the Phase II test was completed and released.

Prior to Phase III testing, described in Test Procedure DTP-097-241-001, modifications to the test apparatus were required to correct the problems encountered during the Phase II test:

1) Loss of seal lubricant into the sodium pool

2) Scoring of the drive rod by the lower guide bushing

3) Configuration of the annulus between the drive rod and the housing did not simulate the current IVTM design

4) Insufficient instrumentation to provide drive rod and housing temperature data for correlating sodium depositions found at the end of the test to the sodium transport analytical model

5) Inability to visually observe the drive rod conditions below the seal housing during the test.

To resolve these problems, the following features were added to the test apparatus:

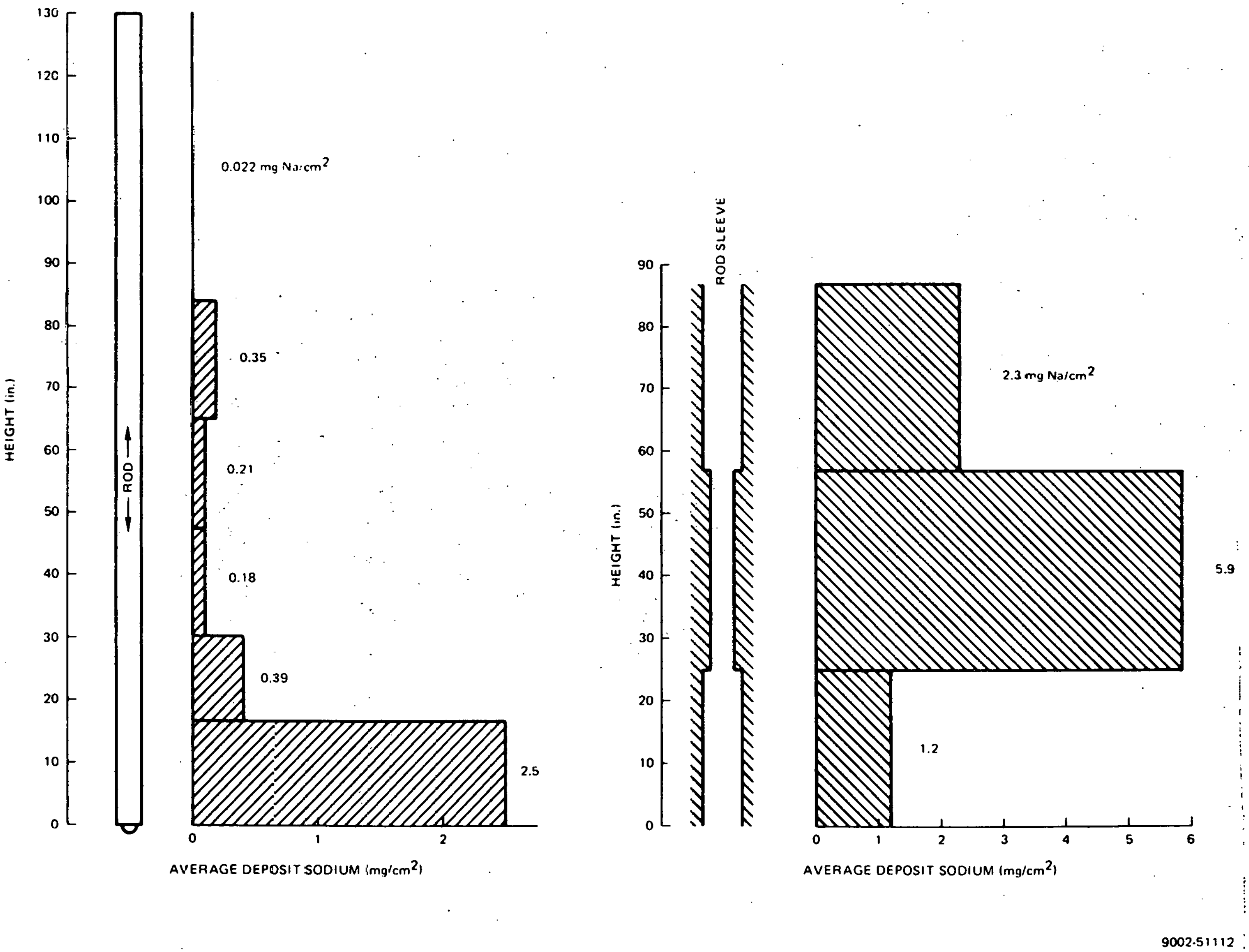

Figure 9. Sodium Deposition on Stem Rod and Sleeve

1) A scraper assembly was added just below the seal housing (refer to Figure 7) to scrape and collect the excess lubricant adhering to the drive rod.

2) The lower guide bushing was redesigned (refer to Figure 5), and AMPCO-18-13, and aluminum bronze material, was substituted for the Stellite No. 6 used in the Phase II test. Fabrication of the roller guide bushing assembly (refer to Figure 6), intended to be used as a backup to the aluminum bronze sleeve bushing, was cancelled at the direction of RRD.

3) The inner wall of the heat apparatus housing, which forms the annulus around the drive rod, was redesigned to simulate the configuration of the current IVTM design.

4) Additional thermocouples were incorporated into the drive rod and on the annulus housing wall to obtain a detailed temperature history as the drive rod was being reciprocated during the test. This provided the data necessary to correlate the sodium frost deposition rates with the analytical model.

5) A viewing port was added, just below the seal housing, to provide the capability for observing the condition of the drive rod and the effectiveness of the lubricant scraper. Inclusion of this feature precluded the necessity of periodic shutdowns to inspect these components.

Based on results of an extensive lubricant screening test, conducted under Task 11, it was decided to use a new grease for lubricating the elastomeric seals. The grease, WSX-8788, is a polyester-base material, made by Exxon. In the lubricant screening tests, the WSX-8788 showed greater compatibility, less weight gain, and caused less hardness to develop, when used with either silicone or EPR elastomers, than did the DC-55M used in Phase II testing.

Phase III tests were also used to qualify seals from a second vendor. These seals were from Parker Seal Co., whereas the seals qualified during Phase II were from Greene, Tweed & Co. Results verified that the Parker seals performed well at the 300°F maximum stem temperature. Seal leakage was only a small fraction of the tolerable limit, and remained almost constant throughout the duration of the test, which encompassed 219,600 ft of stem travel. This was the test goal for equalling 5 years of operation of the IVTM.

The redesigned lower guide bushing of aluminum bronze performed satisfactorily, and caused no scoring of the stem, as was found during Phase II with the Stellite-faced bushing. The new bushing was run submerged in sodium for the major portion of the test, but was also run with the sodium level below the bushing and at ambient temperature, with no sodium present, to simulate conditions that can occur in the IVTM. The bushing and stem suffered no ill effects from either of these conditions.

Results of using WSX-8788 lubricant instead of Dow 55-M were satisfactory during Phase III tests. Deposits of hard, waxy heelmarks on the stem did not occur, but a film of gummy substance was observed on the surface, indicating that the operating conditions were near the upper temperature limit for this lubricant.

The nylon scrapers, added below the seal housing, collected a significant amount of lubricant, and appear to be worth retaining in the final design.

Drag loads were found to vary considerably. No tolerance limit has been set for drag loads, the magnitude of which were to be determined from these tests. Since the drag loads were closely related to lubrication conditions, the lubrication was carefully controlled to maintain sufficient lubricating film without excessive consumption. It was found that adequate lubrication was attained, using a pressure of ~ 10 psi. At 14 psi, lubricant consumption increased considerably; and, at 8 psi, film thickness was marginal, and drag loads increased.

A characteristic trend was observed in drag load, which had a tendency to increase toward the upper portion of the stem travel. This indicated marginal lubrication on the lower portion of the stem, as it moved through the seal housing. This indicated lubrication could be insufficient for the actual stroke length of 18 ft required in the IVTM, since the stem travel used in the test rig was only 5 ft.

The seal housing was modified, so the lubricant could be applied just below the seals, instead of above the seals, which would maintain the stem lubrication for an indefinite length of stem travel during upstroke, and hopefully produce a constant drag load throughout the stroke. The downstroke was not expected to be a problem, since the cooler portion of the stem would retain the lubrication film better.

It was found that the high load spike at the end of the stroke was eliminated by the relocated lubrication groove. The load trace, however, still had a slope for certain portions of the run, whereas, for others, it was level, indicating a constant drag for most of the stroke length. It was discovered that the sloped and level traces were related to angular orientations of the stem, and it became apparent that the stem was bowed, causing highest binding in one specific orientation, and lowest binding at 180° away from this orientation. This also showed that there was misalignment in the guide bushings. The centerline through the upper two nylon guide bushings did not intersect the centerpoint of the lower guide bushing. Both a bowed stem and misaligned bushings must exist to produce variation in binding drag load with orientation. A straight stem in misaligned bushings would produce consistently high drag load, and a bowed stem in aligned bushings would produce consistently sloped drag load at all orientations.

The bolts on the seal housing flange were loosened, to allow the seal housing bushings to self-align with the stem. This showed that the binding essentially disappeared, and the load traces became level for most of the stroke length.

Thus, it was concluded that the location of the lubricant application was not critical, and the apparent problem was due to test fixture imperfections, rather than being inherent in the design. A Phase III test report, TR-097-241-003, was issued at year's end.

A Phase IV test, to determine excess temperature capability of the seals, was begun at year's end. The test was initially set for temperatures of 450, 475, and 500°F, corresponding to an analysis of emergency conditions which could occur with a sodium pool temperature of 500°F. Subsequently, the pool temperature was lowered to 400°F. An analysis (TI-099-241-005) reduced these values to 350, 375, and 400°F. The test is currently proceeding as specified in DTP-097-241-001, Rev B.

2. Subtask B — Ex-Vessel Transfer Machine (EVTM)

All tests planned for this machine were completed or initiated during this fiscal year. The tests are discussed individually in the following subsections.

a. Parametric Heat Transfer Test

The parametric heat transfer test described in AI-AEC-13111 (shown schematically in Figure 18 of that report) continued to completion. The purpose of this test was to determine the importance of various parameters in establishing the type and magnitude of free convection flow patterns that occur in a sodium-filled canister containing a spent fuel assembly. This information was used to improve the analytical model used to predict EVTM heat rejection capability. The apparatus was extensively instrumented with thermocouples and permitted variation of the following important parameters: (1) annulus width between the simulated fuel assembly housing and canister wall; (2) the height of hotter liquid metal above the heated section; (3) height of colder liquid metal below the heated zone; (4) the average temperature of liquid metal inside the fuel assembly housing (hot leg) compared to the average temperature in the annulus (cold leg); and (5) the distance between the top of the heated zone and liquid metal upper level.

Table 3 summarizes the four test configurations used. The last two test series, Configurations III and IV were run using the shell of Configuration I and increasing the diameter of the flow tube to reduce the friction losses, thereby more nearly approaching EVTM characteristics. Configuration IV used a 5/16-in. asbestos tape insulation on the shell to determine the effect of varying radial thermal resistance.

TABLE 3
TEST CONFIGURATION SUMMARY

Parameter	Test Configuration			
	I	II	III	IV
Hot-Cold Leg Combinations Tested (See Figure 17, shown later)	B-F D-G B-H	B-F D-G	B-H B-G	B-G
Flow Tube ID (in.)	1.435	1.435	1.652	1.652
Flow Area in Tube ($in.^2$)	0.467	0.467	0.993	0.993
Annulus Gap (in.)	1.0675	0.505	1.005	1.005
Asbestos Tape Insulation (in.)	0	0	0	0.3125

Figure 10 shows the effect of varying the liquid sodium level for a given hot-cold leg length combination. Raising the level lowered the hot leg temperature only because of the added surface area available for heat transfer. Lowering the level prevented the overall convection loop resulting in less efficient heat transfer and, therefore, higher sodium temperature. The small temperature increase (30°F) shows a very weak loop. The slope of the hot leg temperature was unchanged; therefore, it was deduced that local convection loops in the annulus are not affected by loss of overall convection.

Figure 11 shows the effect of varying the cold and hot leg lengths. Since a strong overall convection loop was not developed, the cold leg acted as a fin and was quite inefficient from a heat transfer standpoint. Local convection loops apparently developed in the annulus, thus maintaining a fairly uniform temperature and resulting in good heat transfer. As a result, the combination BF, having a minimal cold leg, showed the lowest peak temperature. Combination BH had the same hot leg length; however, the longer cold leg reduced the heat transfer efficiency and the peak temperature was raised. Combination DG had a shorter hot leg and longer cold leg than BF. This resulted in less heat transfer area at the high temperatures. This, combined with the less efficient cold leg, resulted in a higher peak temperature. Local convection loops in DG appeared stronger as the slope of the hot leg temperature was lower than that for the BF or BH combinations. This was also due in part to the effective fin length being shorter. In all cases, however, the differences in temperatures were fairly small (~50°F), showing this parameter to have a weak effect on heat transfer.

Figure 12 shows the effect of annular gap variation. This was accomplished by reducing the outer shell diameter from 4 in. to 2.875 in., which reduced the heat transfer area by 40%. However, it was apparent that the increased hydraulic resistance reduced local convection loops since the hot leg temperature slope was increased. Since the annular hydraulic resistance was a very small part of the overall loop resistance, the overall convection loop did not appear to be changed significantly.

The hydraulic resistance of the test apparatus, as designed, was significantly higher than that of the CCP-F/A to be handled in the EVTM. Therefore,

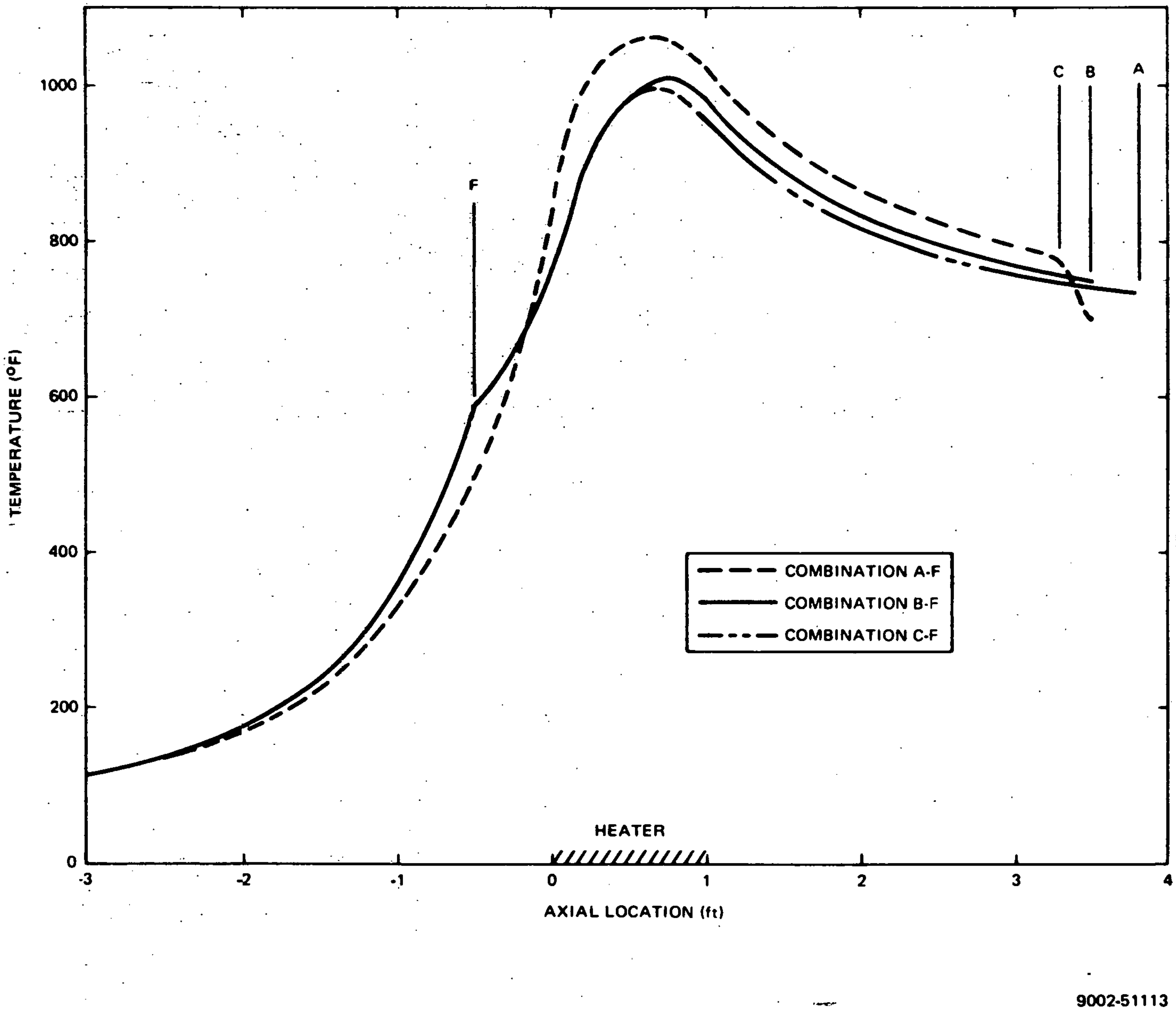

Figure 10. Parametric Heat Transfer Test Liquid Level Comparison

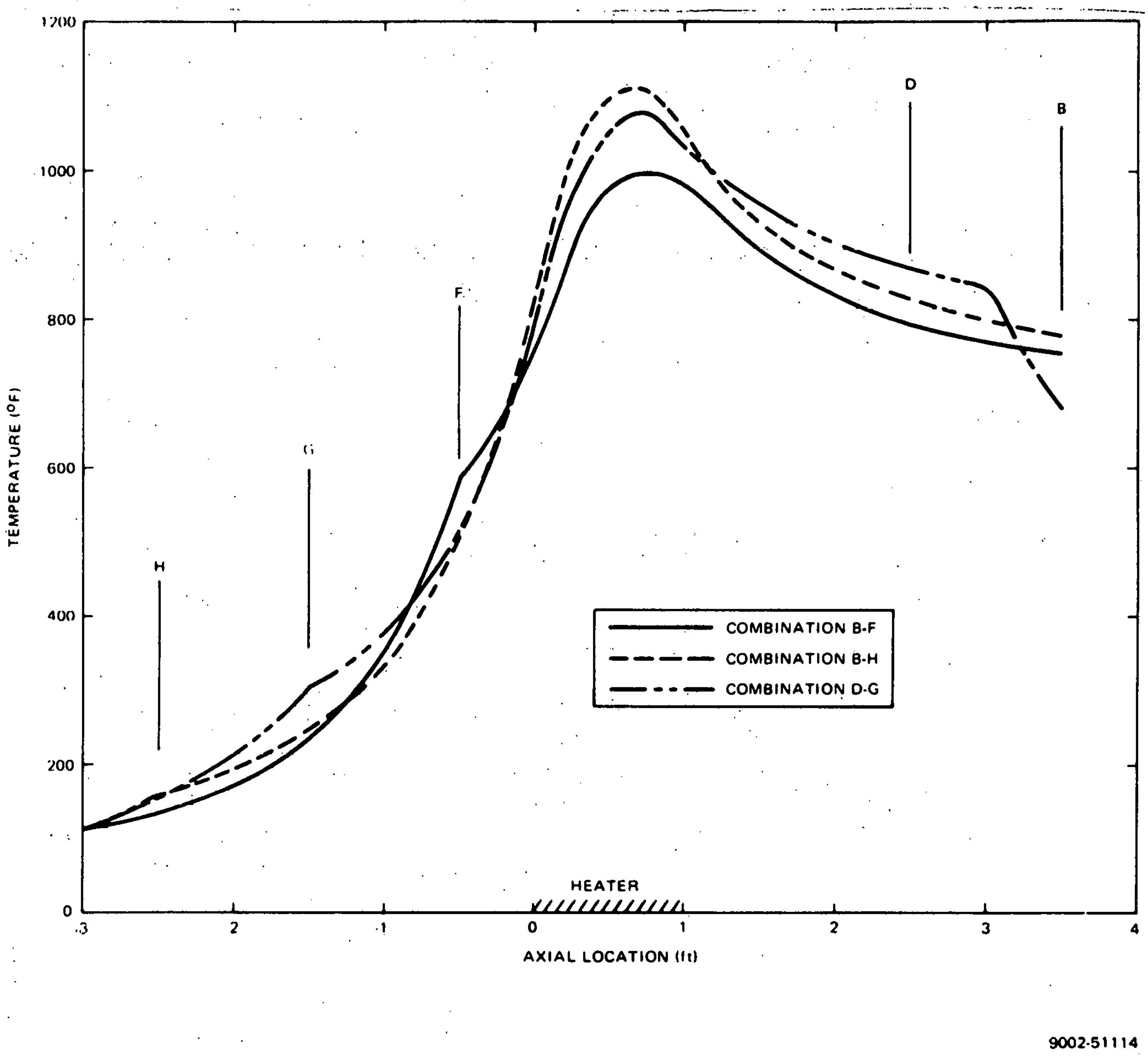

Figure 11. Parametric Heat Transfer Test Hot and Cold Leg Length Comparison

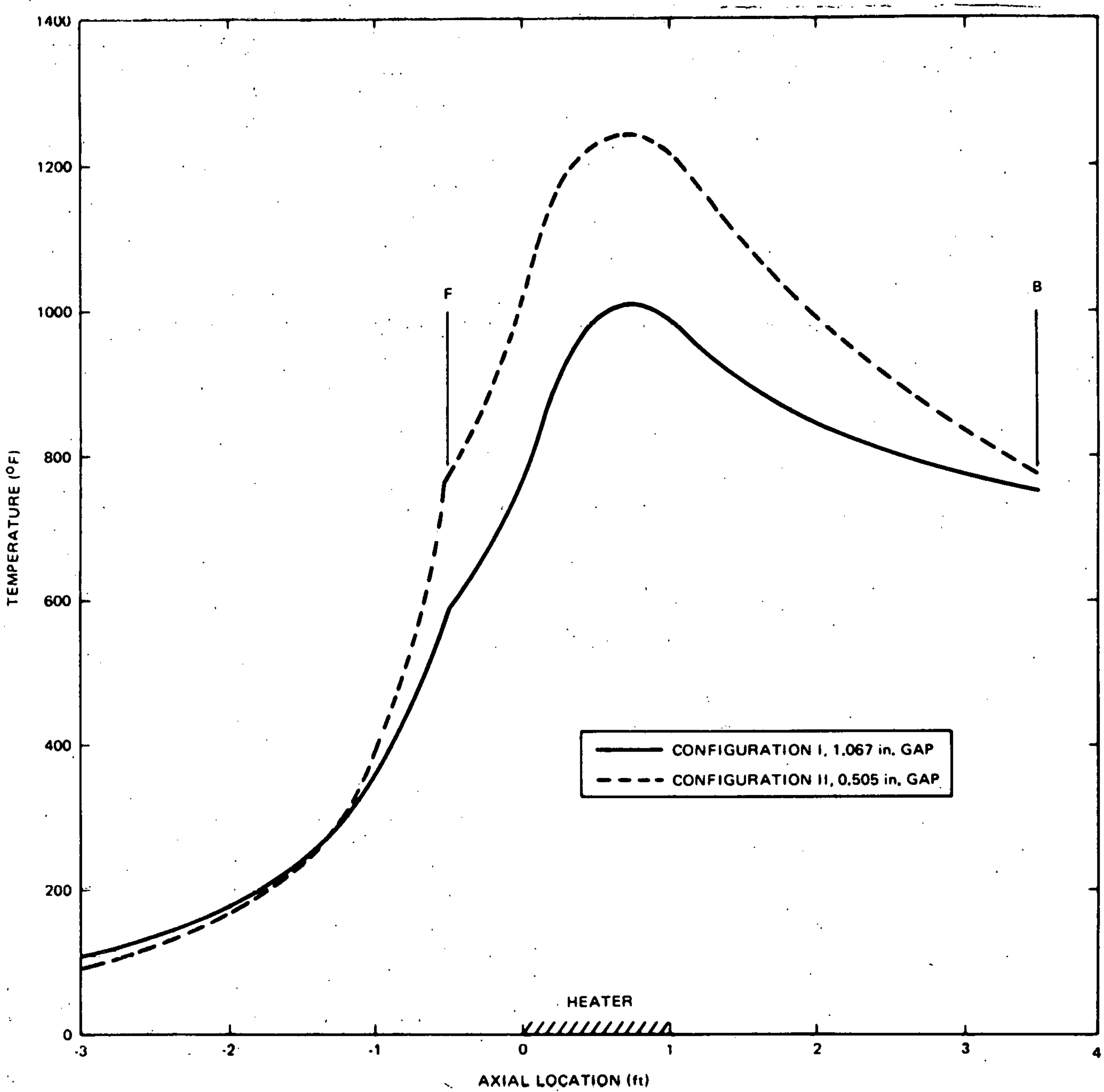

9002-51115

Figure 12. Parametric Heat Transfer Test Annular Gap Comparison

since the reduction of annulus from 1.067 in. to 0.505 in. did not show overall convection improvement, the planned third test series using an 0.3-in. annulus was eliminated in favor of a test using a larger flow tube to reduce hydraulic resistance to match that of the EVTM assembly.

Figure 13 shows the effect of reducing the hydraulic resistance of the overall convective flow loop. The notations "B" and "H" denote the ends of the overall convective flow loop (See Figure 17, shown later). While this configuration change also reduced the annular area, comparison of the profiles indicated that the increase of total loop flow (shown by the higher temperature at "H") offset the decrease in annular flow, resulting in very similar hot leg profiles. The lower temperatures of Configuration III were primarily due to an increase in emissivity, which apparently occurred due to long exposure of the shell at high temperature. This comparison shows the sensitivity of the convective flow to relatively small geometric variations.

Figure 14 shows the effect of increasing radial thermal resistance. Other than the obvious increase in temperature, this parameter appears to have had no effect on convective flow patterns. Because the axial transfer of heat by flow was so much greater than that due to conduction, the effect of the ratio of radial to axial thermal resistance was far overshadowed by this parameter. Since the change from Configuration III to Configuration IV did not involve geometry changes, the flow characteristics remained constant, and the curves are essentially parallel.

In order to duplicate the characteristics of the test apparatus, it was necessary to calculate the wall heat transfer to obtain values of emissivity. Figure 15 shows the calculated overall heat transfer coefficient and Figure 16 shows the calculated emissivity — both as a function of wall temperature. Figure 15 shows remarkably small data scatter with the exception of I BH and the Sub DG series for both annulus gaps. The former was probably an incorrect reading of power. No reason was determined for the high values of U for the Sub DG series.

Because radiative heat transfer is proportional to the fourth power of temperature, calculated emissivity is quite sensitive to the small data scatter of

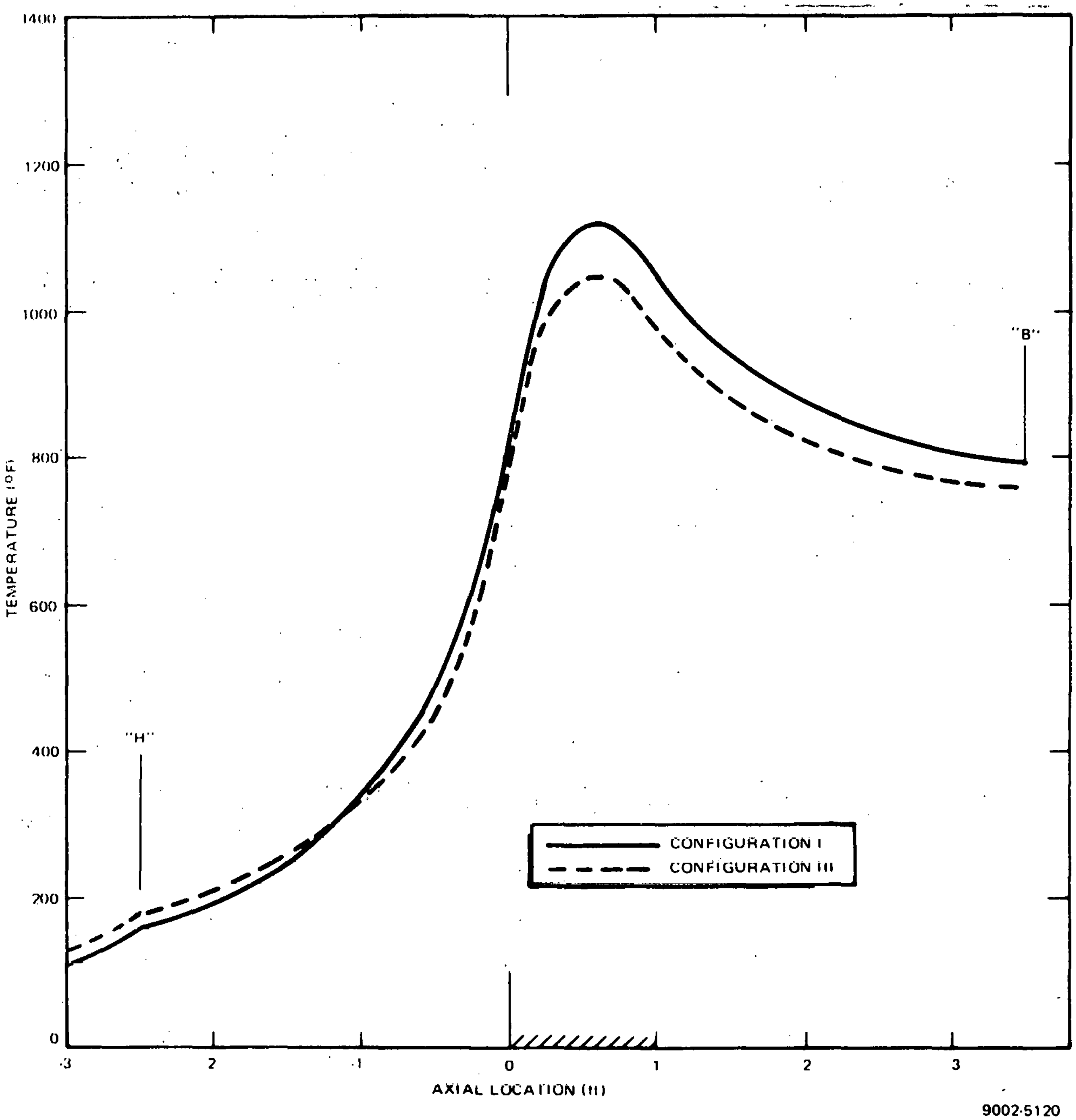

Figure 13. Hydraulic Resistance Comparison (Data for Combination B-H at 4 kw)

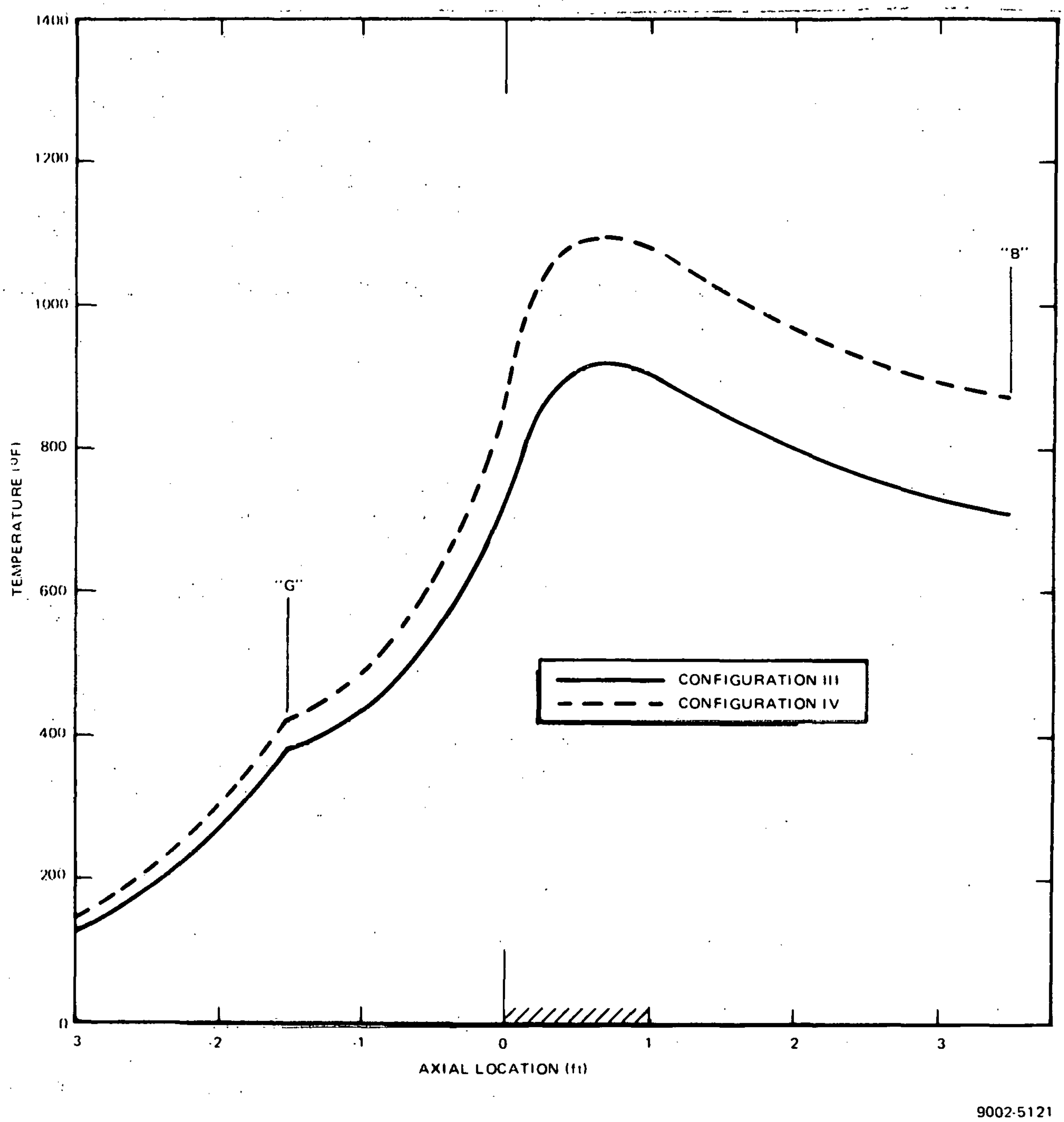

Figure 14. Radial Thermal Resistance Comparison (Data for Combination B-G at 4 kw)

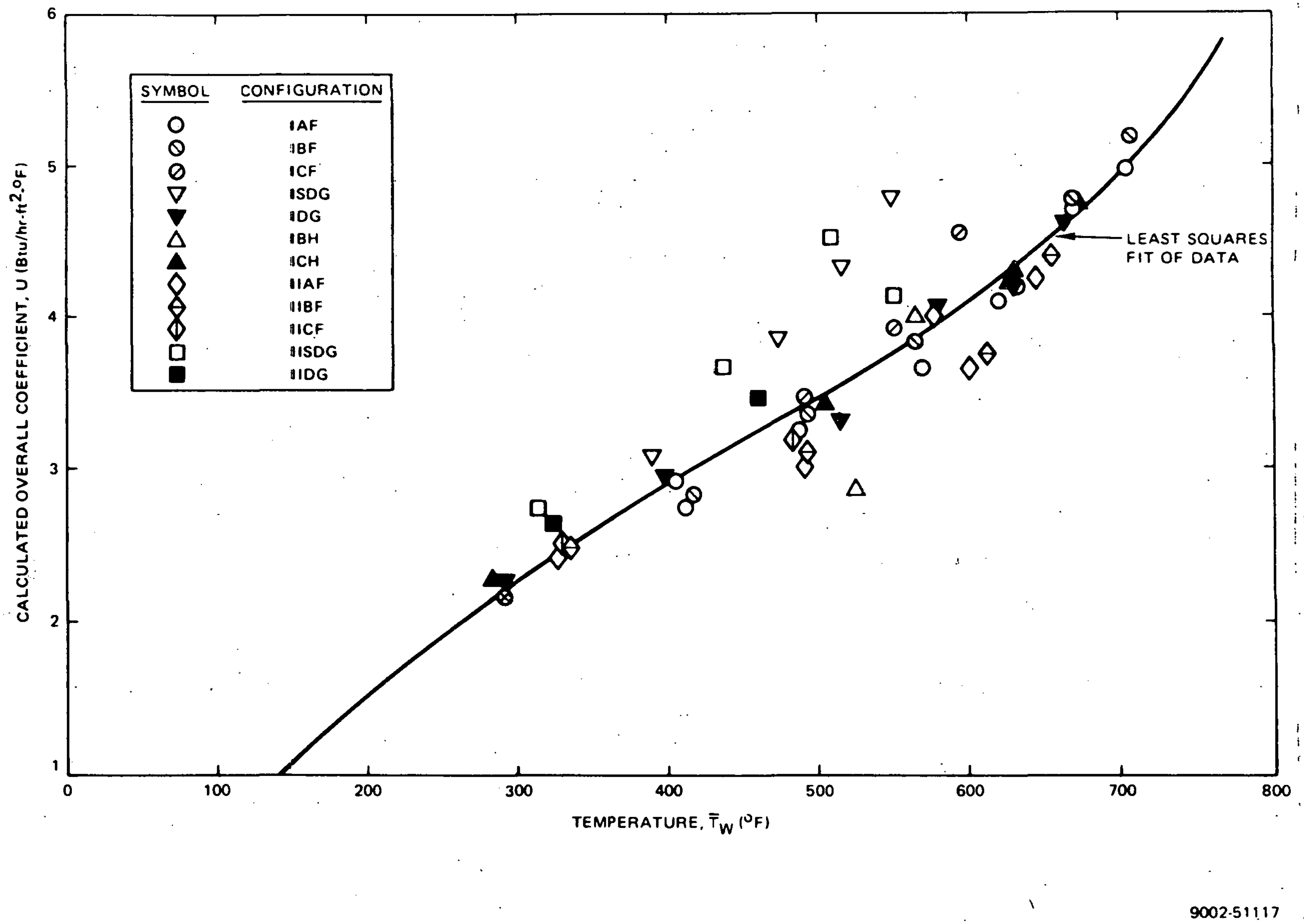

Figure 15. Calculated Overall Heat Transfer Coefficient

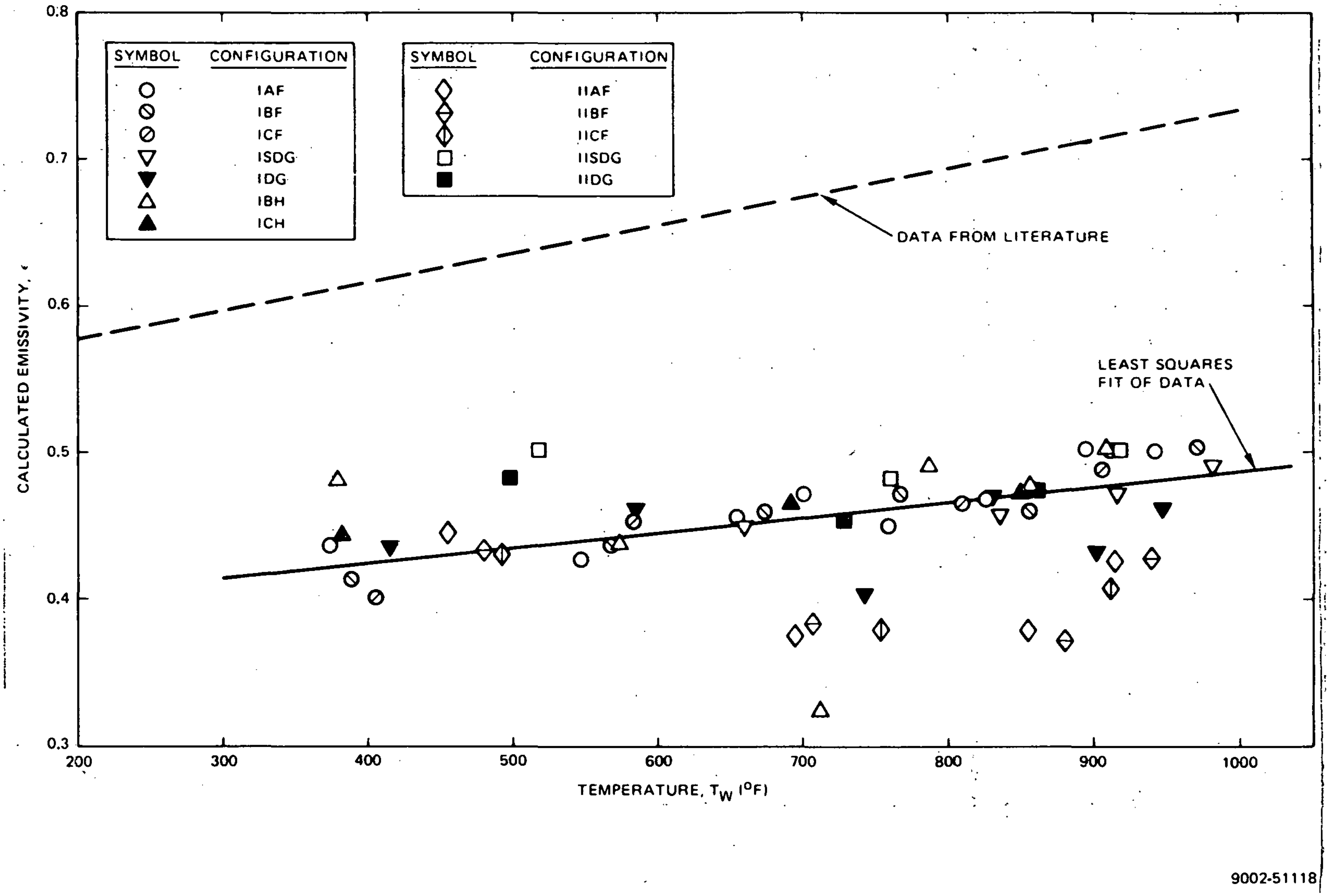

Figure 16. Calculated Wall Emissivity

the overall coefficient. However, the least squares fit to the data appeared to be compatible with the published emissivity values and the service history of the test specimen.

In order to determine the changes required for the theoretical analytical model shown in Figure 17 to match actual test data, trial and error procedure was used to determine the required admittance variation, followed by analysis of the changes to determine the reason for the differences from theoretical. The comparison of the original model showed three major departures from theory:

1) A convection loop exists in the annulus along the hot leg (flat hot-leg profile of test data)

2) The hot leg radial conduction is different from theoretical (ΔT from annulus to flow tube)

3) The overall convection loop is not as strong as theoretical (lower test temperature at "F").

Items 1 and 3 are interdependent. The existence of a local convection loop in the annulus presented a hydraulic resistance to the overall convection loop. Therefore, it was necessary to increase the pressure drop in the overall loop to account for this factor. To simulate the local convection loop, the axial conductance in the hot leg portion of the annulus was increased. The apparent variation in radial conductance was modified by applying multiplying factors to appropriate admittances between the flow tube and the annulus.

Figure 18 shows the comparison of the model with the preceding modifications, the values of which are shown in the figure. This modified model was deemed a sufficient base case to determine analytic techniques to eliminate the use of empirical multipliers.

The three heaters are practically touching the flow tube. As a result, a thermal short circuit exists, and the 20% increase in radial conductivity did not appear out of line. Similarly, in the region above the heaters, the test configuration presented very limited heat transfer paths, considering the tube extensions to have negligible thermal conductivity. Actually, these tubes were packed with boron nitride powder and ceramic standoffs to keep the heater leads

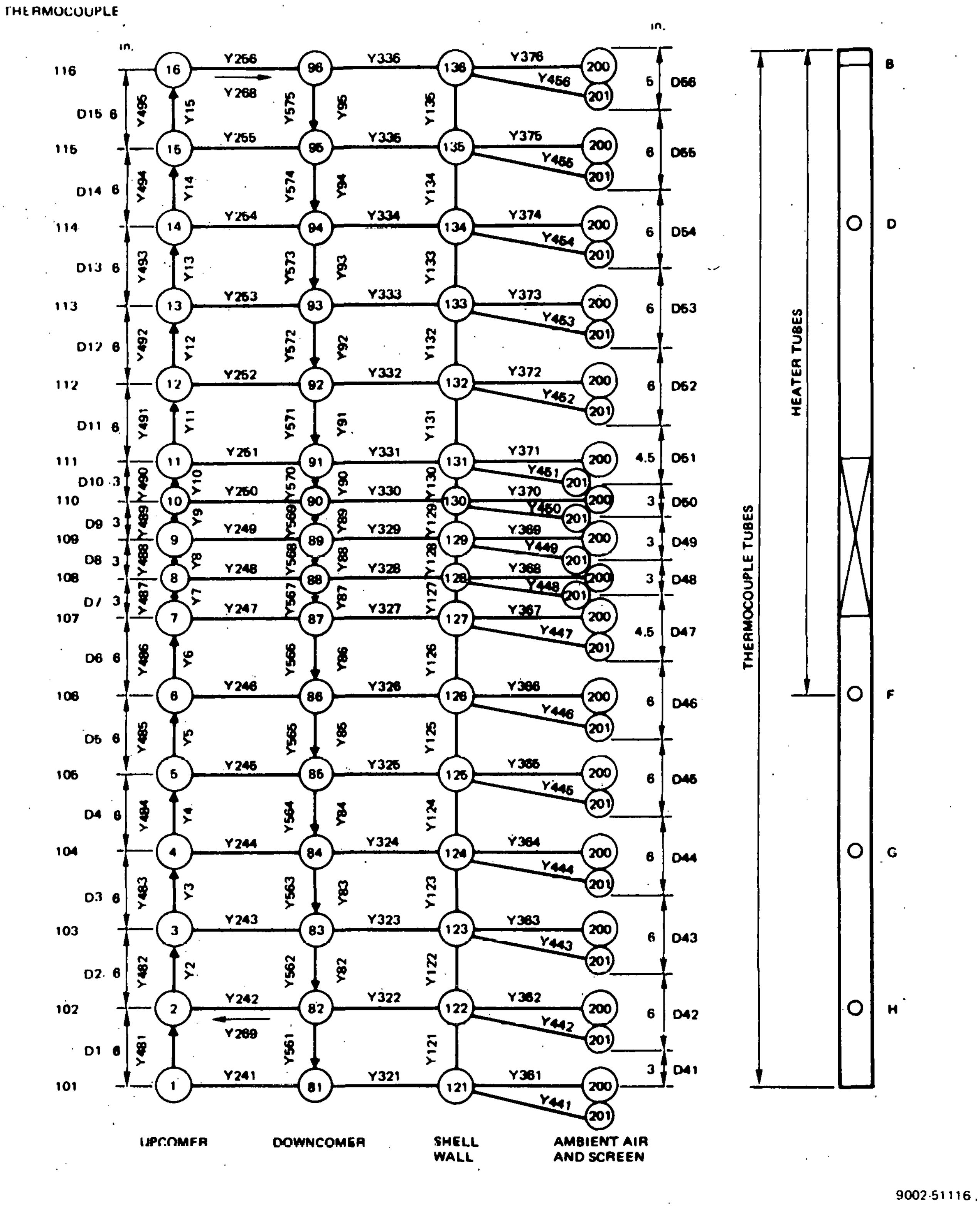

Figure 17. Theoretical Parametric Heat Transfer Test Thermal Analysis Model

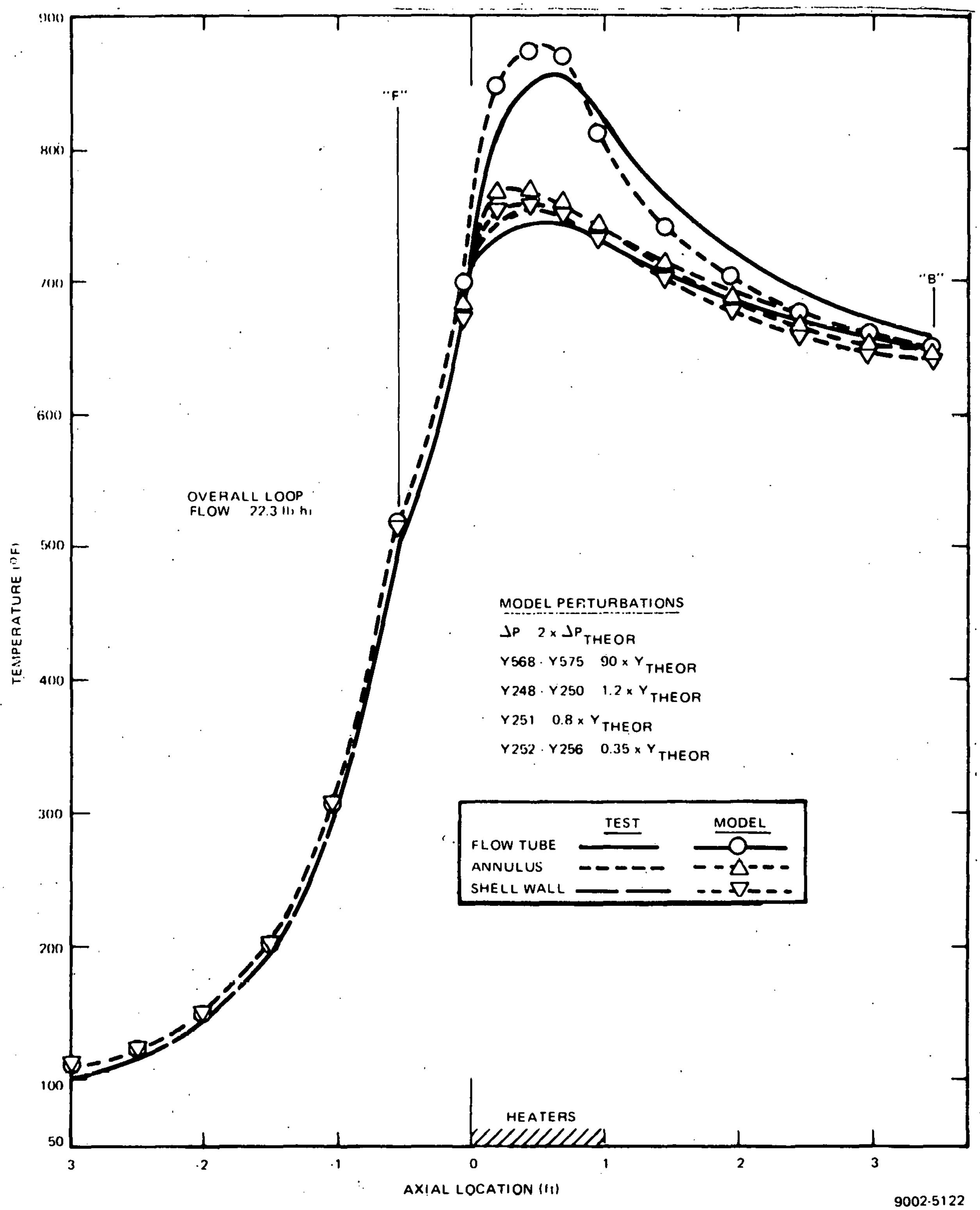

Figure 18. TAP Model – Test Data Comparison – IBF3 (Trial and error admittance variation)

centered. Thus, while solid boron nitride has a fairly high thermal conductivity, the powder packing resulted in a barrier to heat flow, hence the 65% reduction from theoretical.

It should be noted that this condition was peculiar to the test rig, which used a small number of large-diameter heaters. The actual CRBRP fuel assembly, having a large number of small-diameter fuel pins, should approach theoretical values quite closely.

Thus, the only model modifications required to permit accurate matching of (or predicting) test data were the inclusion of the local convection loop and minor radial conduction changes. Figure 19 shows the revised model used to accomplish this calculation. The model assumes the mechanism of flow to be a layer of fluid along the shell wall being cooled and flowing downward. A small portion of the fluid continues to the entrance to the flow tube, and, by natural convection, flows upward to complete the overall loop. The major portion of the downflow is heated as it reaches the heated zone, and reverses direction to complete the local loop in the annulus. The actual flow pattern was probably a series of cascades; however, it is most easily modeled as a single loop.

This revised model was used to model selected runs of all test configurations. The configurations modeled showed excellent correlation.

Although the convection phenomenon is now understood, the emissivity of the CCP and cold wall are unknowns; thus, exact EVTM capability prediction is dependent on a parameter not considered in this test.

The test was deemed successful, and, with the inclusion of the data from the emissivity test (See Section 2-c), very accurate predictions of EVTM and full scale test capability should be possible, using the adjusted analytical model.

Test results were documented in the Test Report (TR-097-242-002) and the Test Analysis Report (TI-099-413-002).

b. Full-Scale Heat Transfer Test

A request for test was issued early in the year delineating full-scale cold wall test requirements. The proposed tests included both transient and steady-state measurements for normal operation, reduced cooling air flow, total loss

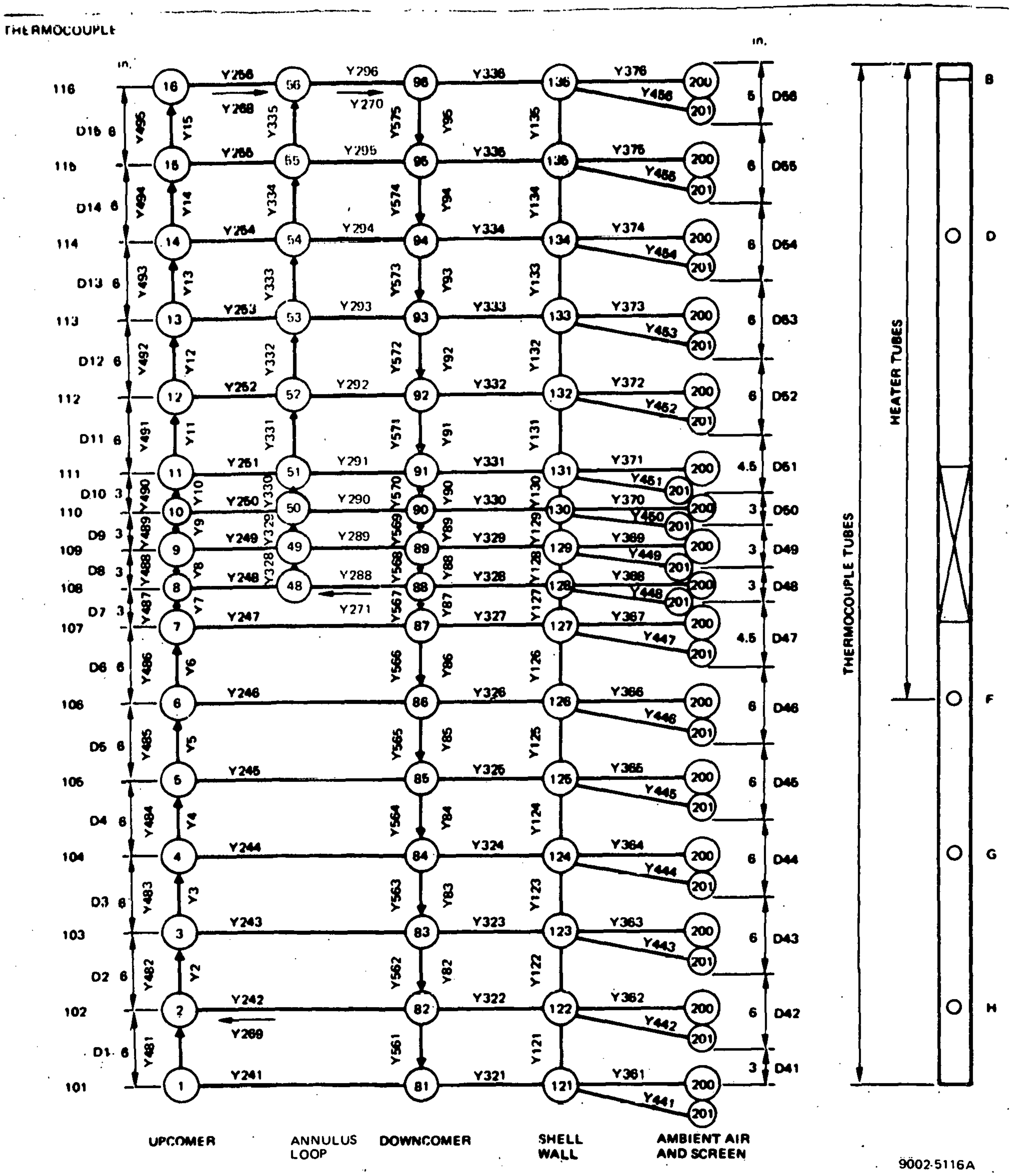

Figure 19. Revised Parametric Heat Transfer Test Thermal Analysis Model

of air flow, loss of sodium in the CCP, overall sodium convection loop blockage, asymmetric fuel assembly location in CCP, and CCP stuck in the uncooled valve stackup. Meetings held with ARD and HEDL personnel indicated that a combined CRBRP/FFTF test conducted at HEDL with AI in the role of monitor-advisor would obtain maximum test data for a minimal cost test.

The basic ground rules for the EVTM-CLEM heat transfer test were agreed upon at an ARD-RRD-HEDL-AI planning meeting in December, and test planning was initiated. The request for test (RFT-099-413-001) (DRS 41.3.01) was revised to reflect compromises made to attain a meaningful combined EVTM-CLEM cold wall test. A series of 27 tests is planned, which includes steady-state and transient runs for normal operation, loss of cooling air, loss of sodium, blocked sodium convection, and one test with a sodium-coated CCP.

The test fixture has been designed to permit dual use in the cold wall and CLEM system tests by using a modular construction. Figure 20 shows the instrumentation and general layout of the test section. The actual test design and planning is being accomplished at HEDL; however, AI is actively assisting in this activity.

The HEDL test plan (TP 41.3.01) was reviewed and approved with relatively minor changes. A conceptual design review was held at HEDL in late February. The design presented was adequate for the test with a few changes required to insure that the test will be as prototypical as possible:

1) A system of thermocouples (TC's) as a backup to ultrasonic level sensing will be used, instead of a gas bubbling system proposed by HEDL, to eliminate a possible cause of flow disturbance.

2) A 12-spoke arrangement of TC and heater leads at the fuel assembly outlet is required to minimize radial flow resistance between the assembly and annulus formed by it and the CCP. The arrangement (Figure 21) requires a transition from the hexagonal array of the rod bundle. This can be accomplished using a drilled guide plate as a forming jig.

3) The air ducting as proposed by HEDL would not have the same hydraulic characteristics as the EVTM cold wall since the plenums used would present no resistance to natural-convection flow.

Figure 20. EVTM-CLEM Cold Wall Test Thermocouple Installation (Sheet 1 of 2)

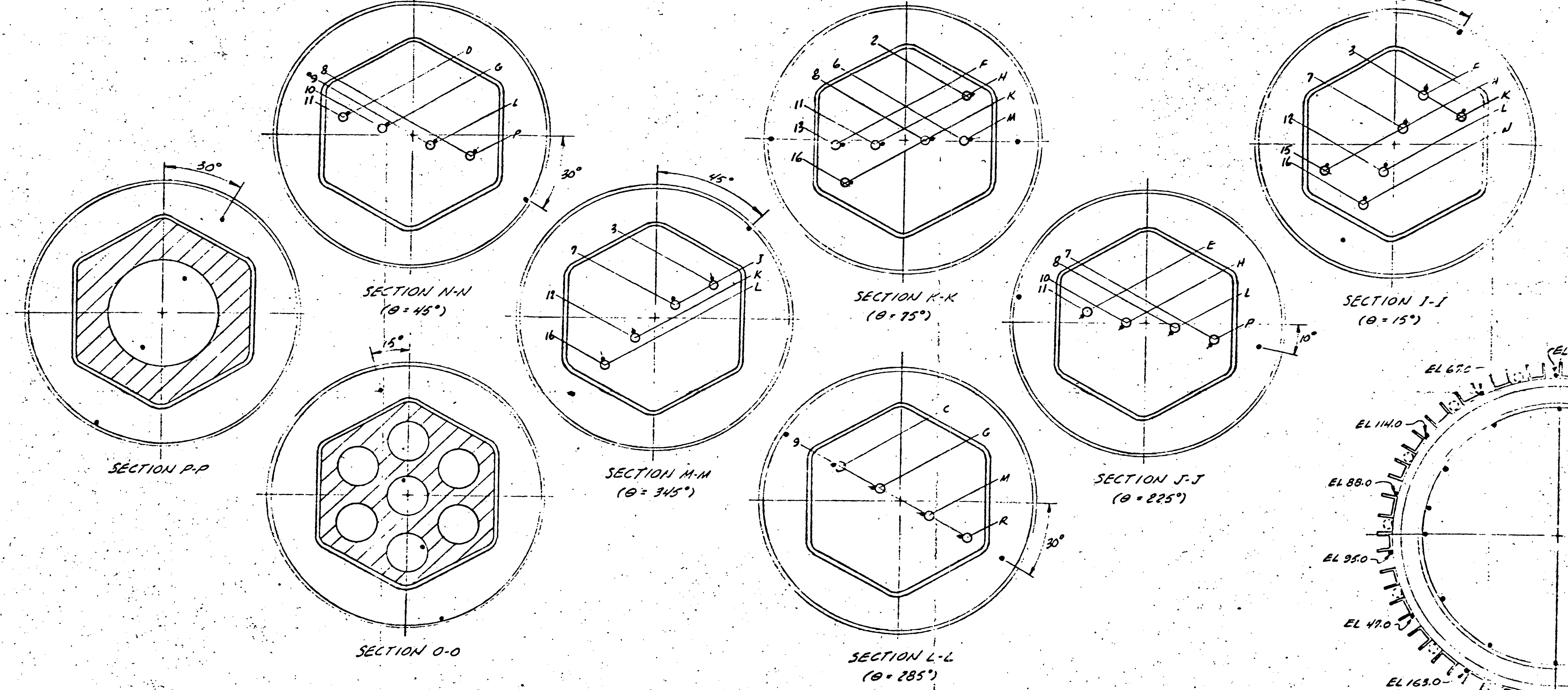

GENERAL NOTES

(1) T/Cs BELOW ROD BUNDLE ARE EXTENSIONS OF WIRE WRAP REPLACEMENTS

(2) WIRE WRAP CW FROM INLET END, 12" PITCH

(3) T/Cs IN ANNULUS MAY BE SUPPORTED FROM EITHER CCP OR DUCT, CENTERED BETWEEN SURFACES

(4) HEATER & T/C LEADS EXIT THROUGH OPENINGS ON OUTER PERIMETER OF UPPER SHIELD BLOCK & HANDLING SOCKET MOCKUP (SECTIONS O-O & P-P)

(5) 99 T/Cs DISTRIBUTED AS FOLLOWS:

- 53 - ROD BUNDLE & INLET
- 4 - UPPER SHIELD & SOCKET
- 28 - ANNULUS & CCP WALL
- 14 - COLD WALL

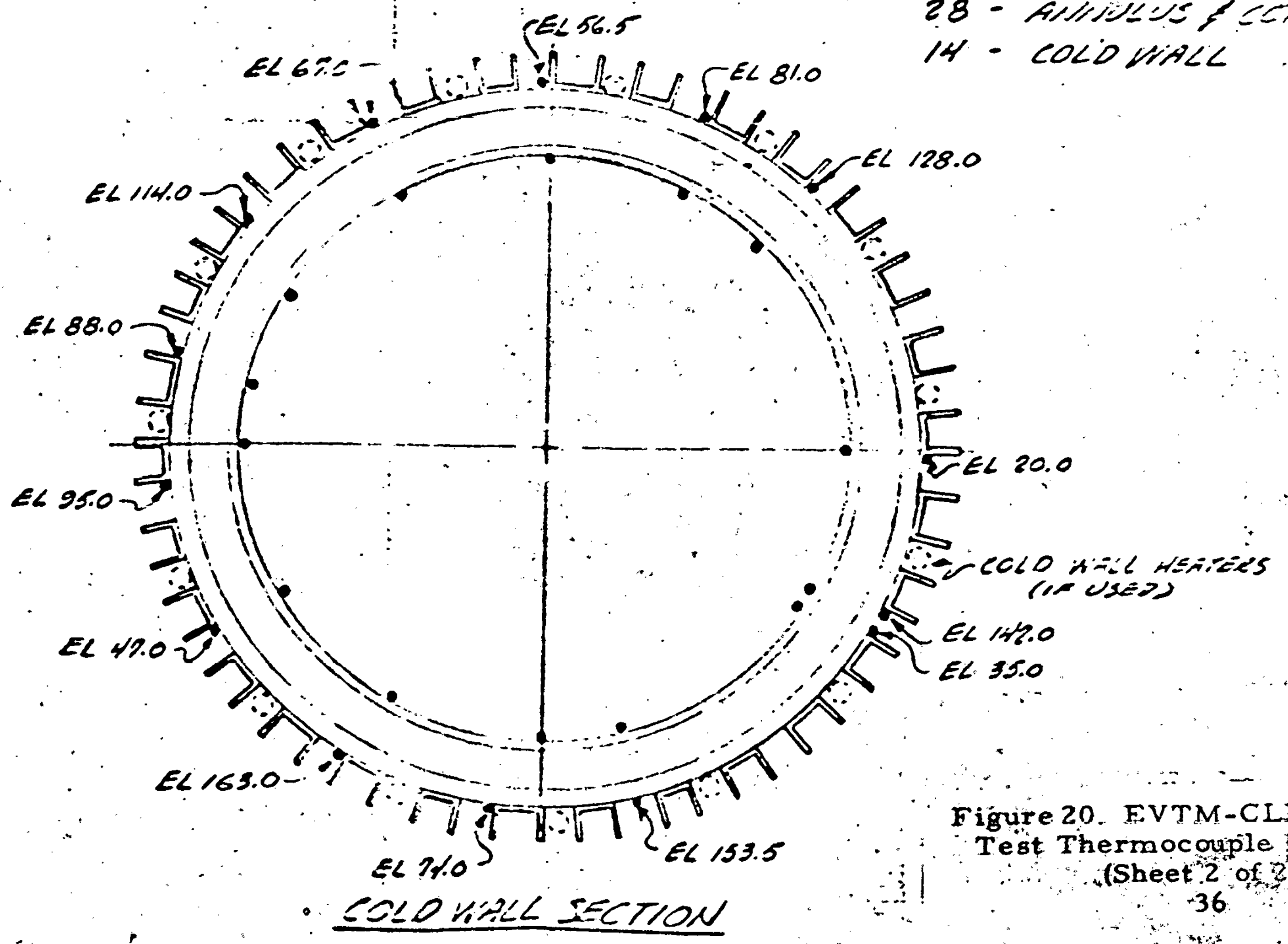

Figure 20. EVTM-CLEEM Cold Wall Test Thermocouple Installation (Sheet 2 of 2)

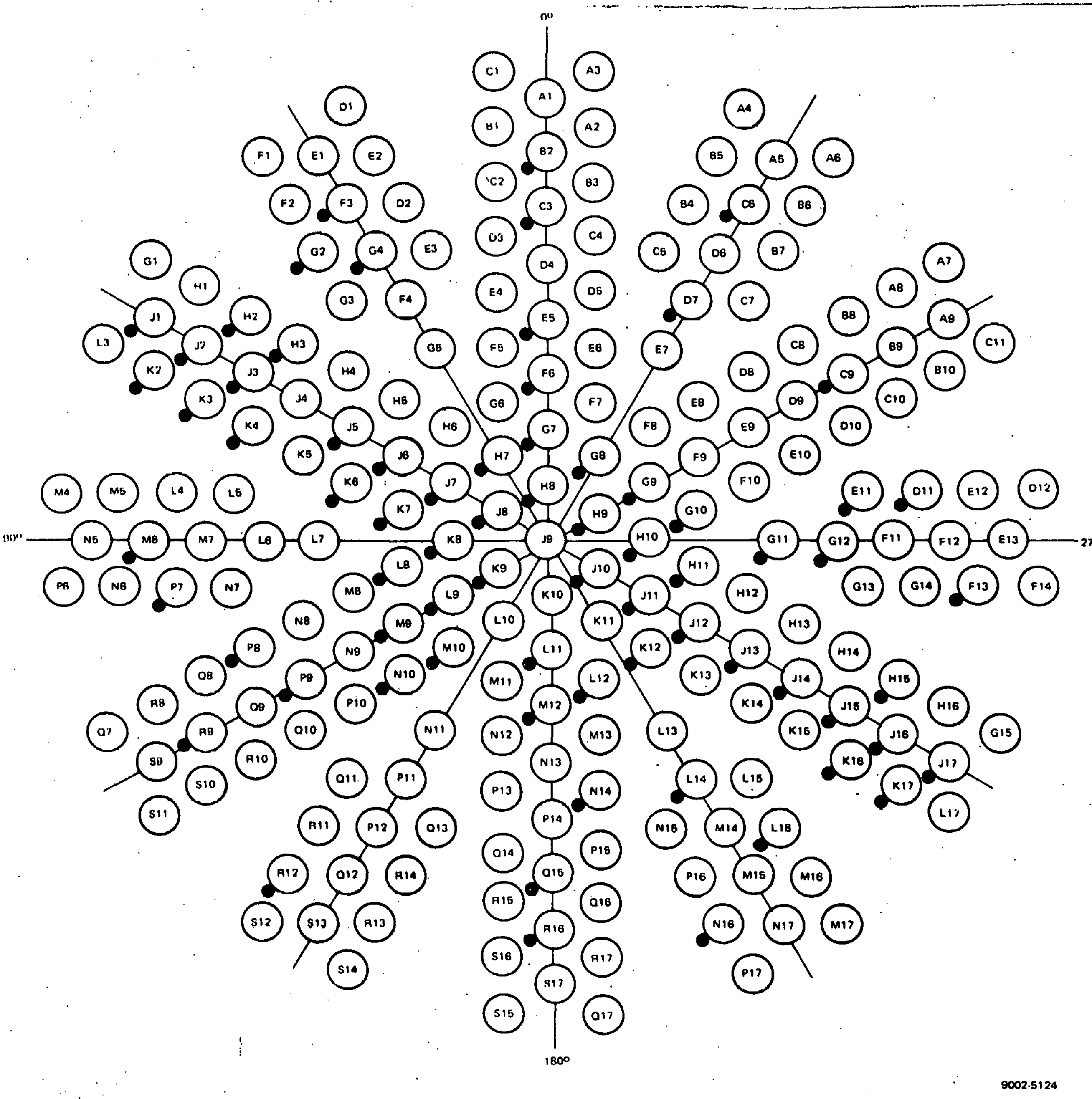

Figure 21. Heater Lead Identification

A final design review was held in mid May and the design was approved by AI and ARD with very minor modifications. Subsequently, Acro-Tech Machine Co. of Gardena, California, was awarded the contract for fabrication of the electrically heated fuel bundle. Fabrication completion now appears to be at the end of July 1974. Bids and/or purchase orders have been released on the cooling air shroud, CCP mockup, electrical equipment and air ducting. The coated cold wall and spare CLEM blower are at the test site.

The analytical model for predicting test results for use as a guide in defining specific test procedures has been formulated and is being checked out. The model is shown in Figure 22.

c. Emissivity Testing

The EVTM uses the cold wall method of heat transfer, i.e., an annular region cooled by forced air, with the decay heat of the fuel assembly immersed in a sodium-filled CCP transferred to the air by conduction and radiation through the argon cover gas. Of these modes, radiation is most important (~85% of the heat transfer); and as a result, testing was initiated to determine the emissivities of the CCP and cold wall. Two tests are underway to accomplish this: a subscale test to determine realistic effective emissivities between the two surfaces, and a coupon test to determine absolute limits of surface emissivities.

The subscale test plan (TP-097-242-002) was completed and released. Layout and subassembly drawings are complete. Figure 23 shows the layout of the test assembly. The final assembly and test modification drawings have been initiated. A vendor has been located with the capability for applying a black chrome emissivity coating to the 2-in. pipe cold wall mockup. A report (TI-099-413-006) was issued describing the analytical model to be used for back-calculating emissivity. The model (Figure 24) was used to predict temperature distributions to define test power and times required to simulate EVTM operation. The power ratio is approximately 1/30, and the time ratio is approximately 1/6. The design provides a CCP-fuel assembly model that can be immersed in and withdrawn from a sodium pool, providing maximum simulation of actual EVTM operation. An electrically driven chain mechanism (the IVTM seal and bushing test mechanism, modified) provides vertical motion of the assembly. Sufficient instrumentation is provided to permit analytical modeling to back-calculate emissivity.

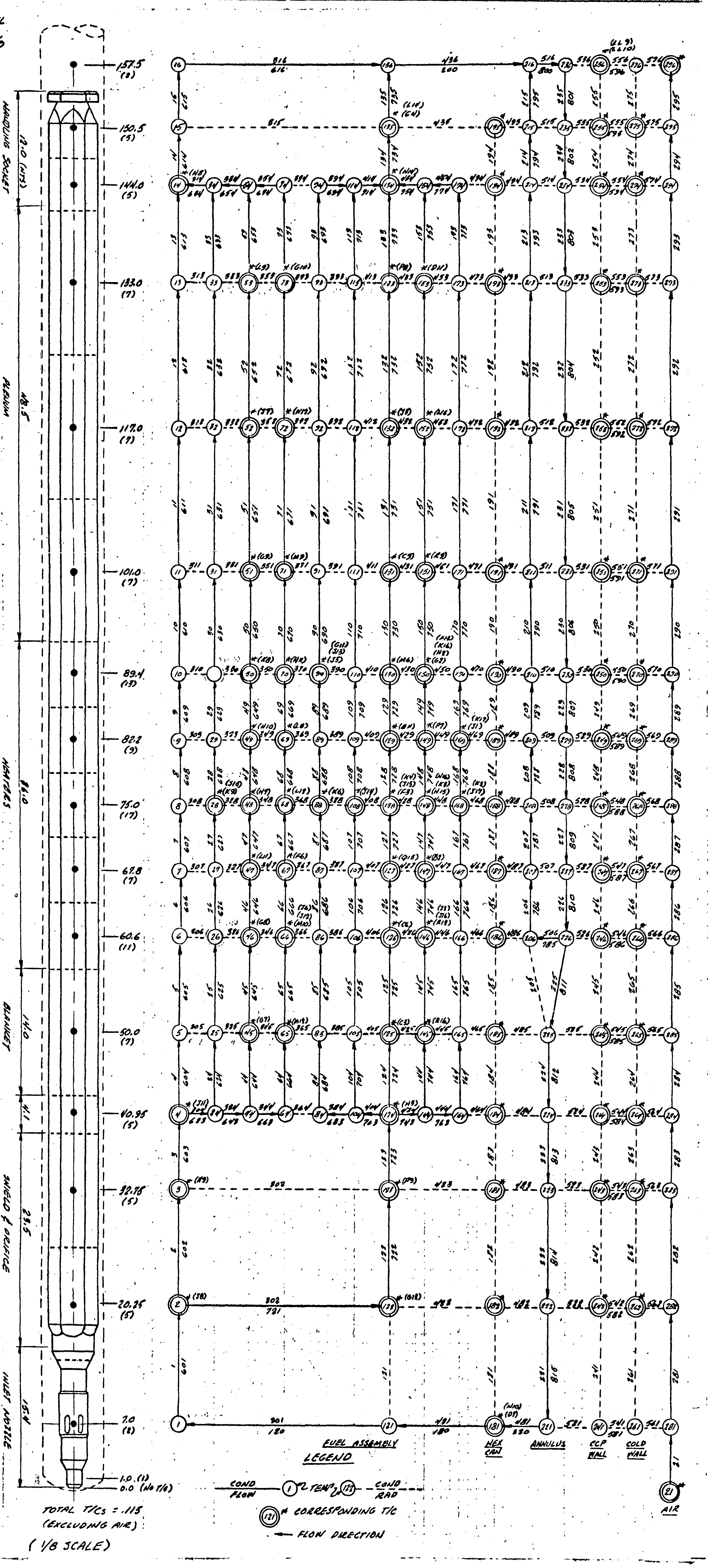

Figure 22. Full Scale Cold Wall Test Model

Figure 23. Subscale Test Layout (Drawing No. EX-N099413005)

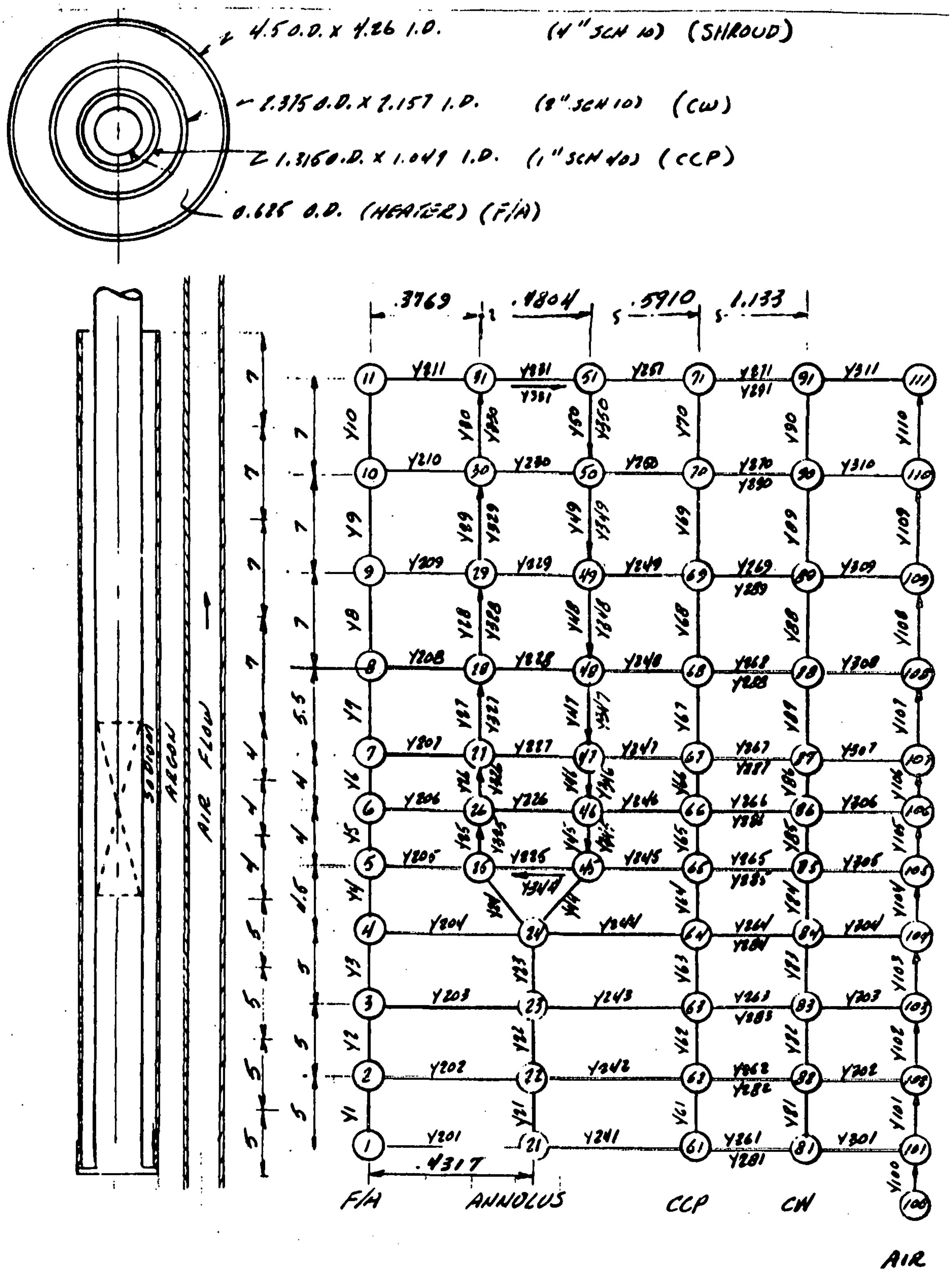

Figure 24. Subscale Emissivity Test — Analytical Model

The coupon test plan is complete and ready for issue. The test fixture layout drawing is shown in Figure 25. The design is oriented toward use of much of the material purchased for the cancelled FFTF sodium vapor reciprocating seal test. Purchase orders for long-lead items, such as sapphire and potassium bromide viewing windows and radiometer detection systems, have been issued in order to maintain test schedules. Close liaison is being maintained with the subscale test to assure uniformity and maximum equipment usage.

d. Grapple Chain Sodium Immersion Test

Based on the evaluation of the shortened EVTM, a request for test (RFT-099-413-004, DAD 41.3.04) of a crane-type chain was issued. Seven types of grapple suspension members, ranging from tape to roller chain, were evaluated. A crane-type chain was selected for testing. Approximately 14 ft of chain will be immersed in sodium to simulate the reactor pool. The wetted chain travels through the grapple drive system and into the chain fall. Both chain and tape will be tested simultaneously, as shown in Figure 26.

It was learned that equipment suitable for this test was available as salvage from the Fermi I plant. Use of this equipment resulted in substantial cost savings and schedule maintenance.

The Fermi equipment — tape and chain drives and associated controls — have been acquired, and purchase orders for chain and tape have been issued. The test plan (TP-099-413-001) was completed and released. Layout drawings of the test fixture and facility modification are ~80% complete. A study was made to determine the method to be used to increase the sodium loop storage capacity to that required to simulate CRBRP pool conditions. An additional parallel storage tank has been ordered to accomplish this requirement.

e. CCP Syphon Test

Sodium overflow from a CCP in the EVTM during a normal refueling cycle was evaluated to determine the adequacy of the drip pan capacity. The results indicated that for a normal refueling cycle, performed at 33-1/3% handling efficiency, where the 102 spent fuel assemblies each have a decay power of 10 kw, the total sodium overflow would be 7248 in.^{3}. This overflow volume

Figure 25. Coupon Test Layout (Drawing No. EX-N099413037)

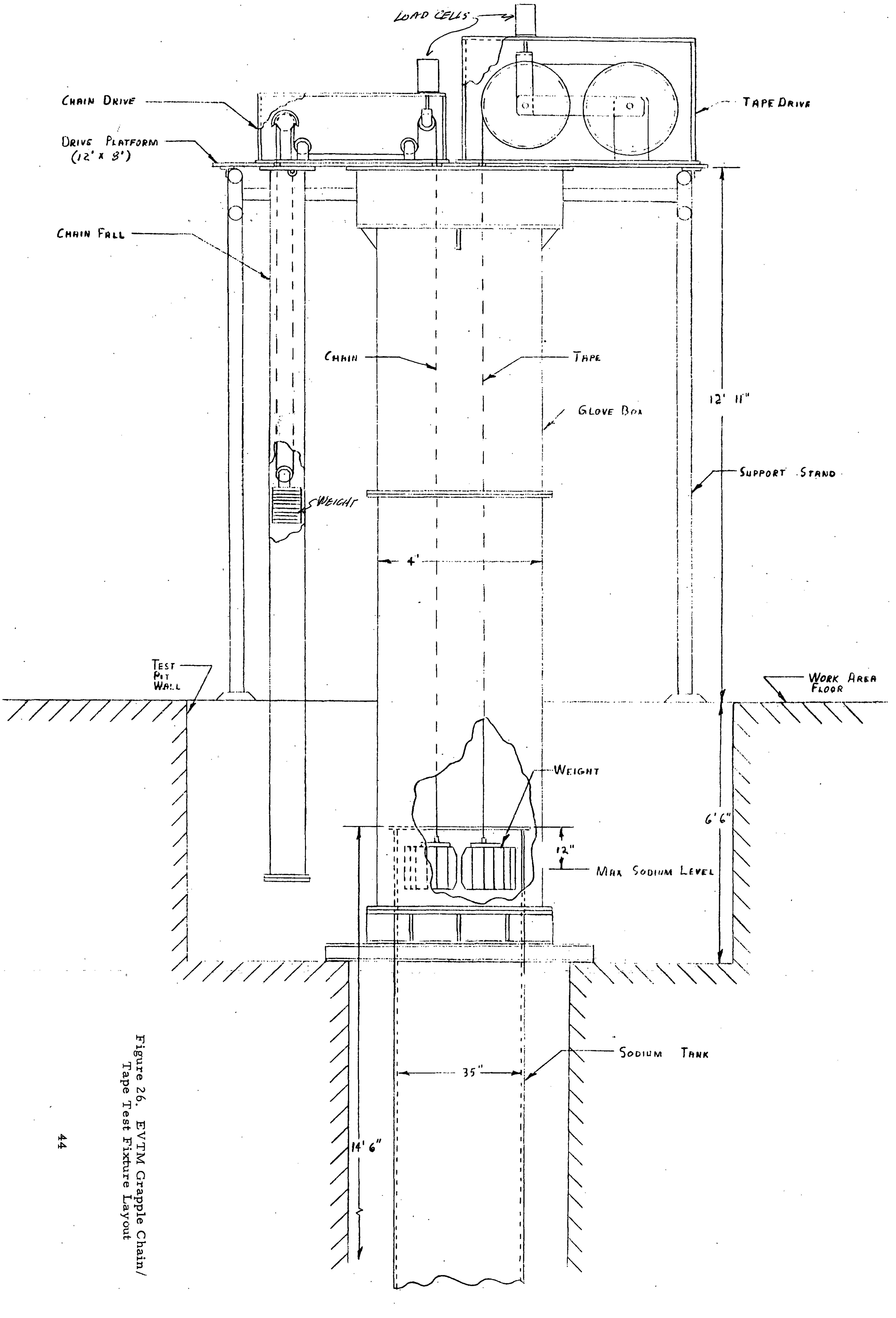

Figure 26. EVTM Grapple Chain/
Tape Test Fixture Layout

would require 7 drip pan changes per refueling based on a 3-pan design with 360-in.^{3} capacity each. In the event that the 102 spent fuel assemblies were transferred, each with a decay power of 20 kw, it was calculated that 13,062 in.^{3} of sodium would overflow the CCP's. This would result in 12 drip pan changes per refueling. These results were based on a transient solution of a thermal model that includes heat transfer to the reactor port, valve stackup, EVTM cold wall, and EVST entry port at appropriate times. If a syphon is not used in the CCP, even with 12-in. longer drip pans in the EVTM, it would be necessary to empty each of the 3 drip pans 4 times during a normal refueling. Therefore, a syphon in the CCP was deemed necessary and a test was required to demonstrate the validity of the concept.

The test plan is complete and ready for issue. The test will use water at 145°F to simulate hydraulic characteristics of sodium at 400 to 500°F. Two design concepts will be tested, with provision made in the test article for easy modification to reflect design changes necessitated by test results.

3. Subtask C — Ancillary Equipment

Activity in this subtask was limited to studies to determine the testing required. Two reports were issued — TI-099-411-010 and AI Letter 74 AT3736. The first described potential plutonium contamination problems during refueling and the second examined the use of the FFTF-IEM all mockup for CRBRP requirements.

The plutonium problem, although an overall plant problem, is primarily manifested in the EVTM refueling operations. Therefore, a request for test (RFT-099-413-007, DAD 41.4.01) was issued to determine methods of handling the problem.

The IEM cell usage was deemed impractical from the standpoint of schedule conflicts and incompatibility with CRBRP requirements. Therefore, a request for test (RFT-099-411-001, DAD 41.4.03) was issued to satisfy the needs of the CRBRP.

4. Subtask D — Refueling System Engineering Studies

a. Alternate IVTM Trade Studies

Alternate IVTM concepts were studied in an attempt to reduce the height of the machine above the reactor head. These studies were restricted to straight push-pull IVTM concepts. The concepts investigated had to satisfy the same requirements as the reference IVTM concept and the reactor core design as of October 1, 1973.

Based on the preceding criteria, the following alternate concepts were selected for study:

1) Ball Screw Driven Grapple Concept — This concept utilizes a ball nut-screw in the reactor cover gas region to vertically displace the grapple. Grapple rotation and grapple finger activation are accomplished by a system of concentric shafts, housed within the ball screw. Each shaft can be independently rotated, relative to the ball screw, when grapple rotation or grapple finger activation is required. The holddown and identification system drives and the core component centering mechanism are identical to the reference IVTM.

   The overall height of this concept is ~16.5 ft above the reactor head (compared to 34 ft for the reference IVTM). The drive section package is about 22 in. wide, 22 in. deep, and 48 in. high. The in-vessel section extends ~13.5 ft above the reactor head, and the maximum diameter penetrating the small rotating plug will be ~18 to 20 in. If the IVTM diameter required is >18 in., then redesign of the small rotating plug port will be required. The concept is not sufficiently detailed, at this time, to accurately establish the IVTM body diameter. A separate structure, containing the service equipment, is required to provide electrical and pneumatic services for the IVTM. This structure is mounted on the small rotating plug, adjacent to the IVTM, and also provides access to the IVTM drive section for installation and adjustments.

2) Chain Pull-Weight Push-Driven Grapple Concept — This concept utilizes a chain hoist within reactor cover gas containment, similar to FFTF, to provide a pull force on the grapple. Push force is provided by the weighted grapple. The pull force is 5,000 lb, and the push force is ~2,500 lb. Grapple finger activation is accomplished by displacing the grapple finger chain relative to the grapple chains. When the grapple is in the fully raised position, a gear face on the grapple

engages a drive pinion which rotates the grapple for core component identification and orientation. The holddown and identification system drives and the core component centering mechanism are identical to the reference IVTM.

The overall height of this concept is ~ 15.5 ft above the reactor head. The gear box containing the chain sprockets and motors measures ~65 in. in diameter, and is ~ 80 in. high. The overall drive section package, including structural supports and chain fall housing, measures ~ 65 in. in diameter and 153 in. high. The in-vessel section extends ~ 10 ft above the reactor head, and the maximum diameter would be >18 in., which requires redesign of the small rotating plug port. A portable service platform for mating the IVTM drive section to the in-vessel section is required for this concept, and a clean, reactor grade, argon gas supply is required to purge the IVTM during operation.

Layouts of these concepts were prepared (AI Drawings R-N099412009 and R-N099412010), and were included in the refueling task force trade study report (TSR-099-410-001).

These concepts were evaluated with respect to the reference rising stem IVTM concept. The comparison showed that the reference concept was easiest to maintain, had the least impact on schedule, had greater reliability, resulted in the smallest downtime penalty for installation and removal, and fit within the current port size of the small rotating plug. These considerations led to the conclusion that the rising stem IVTM should continue to be the reference concept for the CRBRP. The recommendation was made, subject to the following assumptions:

1) That the seismic loads imposed on the small rotating plug do not significantly affect the small rotating plug bearing design, nor its capability to react to the IVTM-imposed seismic loads (an analysis of the IVTM seismic loads was performed, TI-099-412-005, and submitted to ARD for evaluation).

2) That the shield temperature will not significantly affect the capability for maintaining the grapple rod temperature, passing through the reciprocating seals, below 300°F. (See Phase IV Seal and Bushing Test, Section II-B.1.a.)

3) That the gantry width can be reduced to avoid interference with the IVTM, regardless of IVTM height changes. Discussions with the FFTF gantry manufacturer indicated there should be no problem in doing this.

b. Shortened EVTM Study

A concept of a shortened EVTM was prepared for evaluation. The reference EVTM utilizes the basic FFTF CLEM design, as much as possible. The reference EVTM only requires two changes to the CLEM design: (1) increase the capacity of the drip pans, and (2) increase the valve extender stroke from 4 in. to 9 in. to facilitate cleaning and decontamination. The short EVTM utilizes a shortened (1000-lb push capability) grapple. The grapple, plus the 190-in. long CCP established the basic machine internal cavity height.

Figure 27 shows the heights of the long and short EVTM's. The weights of the EVTM's are 232 and 190 tons respectively. The shorter EVTM would withstand greater seismic loads than the longer one. Approximately 18 ft of the grapple chain would be in sodium in the reactor. The wetted chain, with the grapple up, traverses the grapple drive into the chain fall.

A conceptual sketch (Figure 28) was prepared of the shortened EVTM. This concept utilizes a crane chain hoist system. An alternate tape drive concept was also prepared, as shown in Figure 29. The selection of a chain versus a tape grapple drive system will depend on results of tests to be conducted under Subtask B.

The EVTM height reduction allows reduction in either the number or length of cask body modules. Reducing the number of cask body modules is more cost effective than shortening the modules as less machining is required. The concept utilizes four modules, a reduction from seven to four.

The EVTM height reduction allows reduction in the gantry height. Clearance under the gantry girders was originally established at 19 ft to clear the IVTM drive section. Increases in the required IVTM stroke increased the IVTM drive height such that the gantry girders were moved closer together to provide a clearance between the girder and the IVTM drive. This change, in conjunction with the short EVTM, allows the clearance under the girders to be lowered. An 8-ft clearance has been arbitrarily established for personnel safety, as shown in Figure 30.

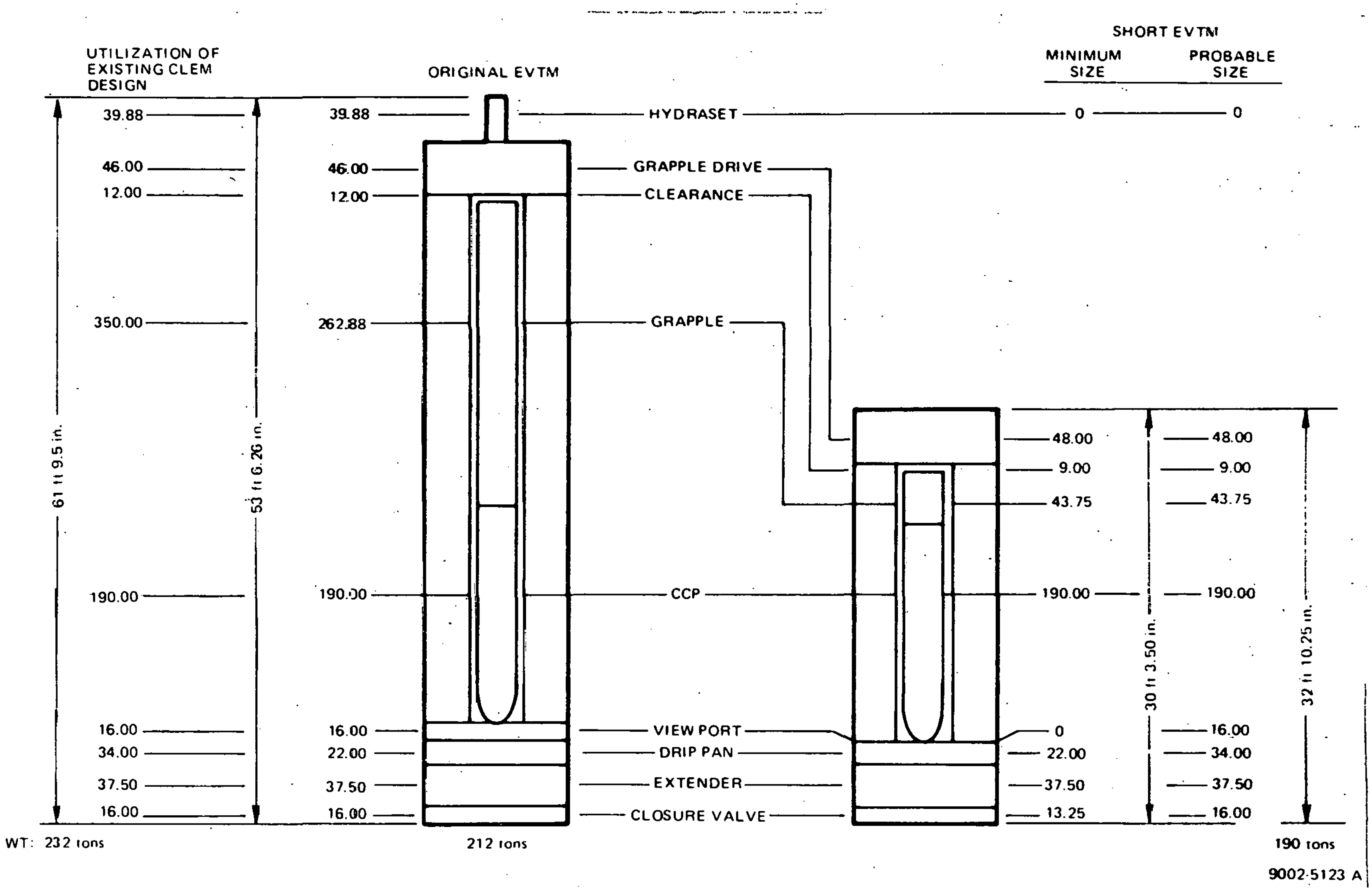

Figure 27. Reference Cold Wall EVTM Length Reduction

Figure 28. CRBRP Conceptual Ex-Vessel Transfer Machine (Drawing No. N099413013)

Figure 29. Grapple Control Mechanism Tape Concept

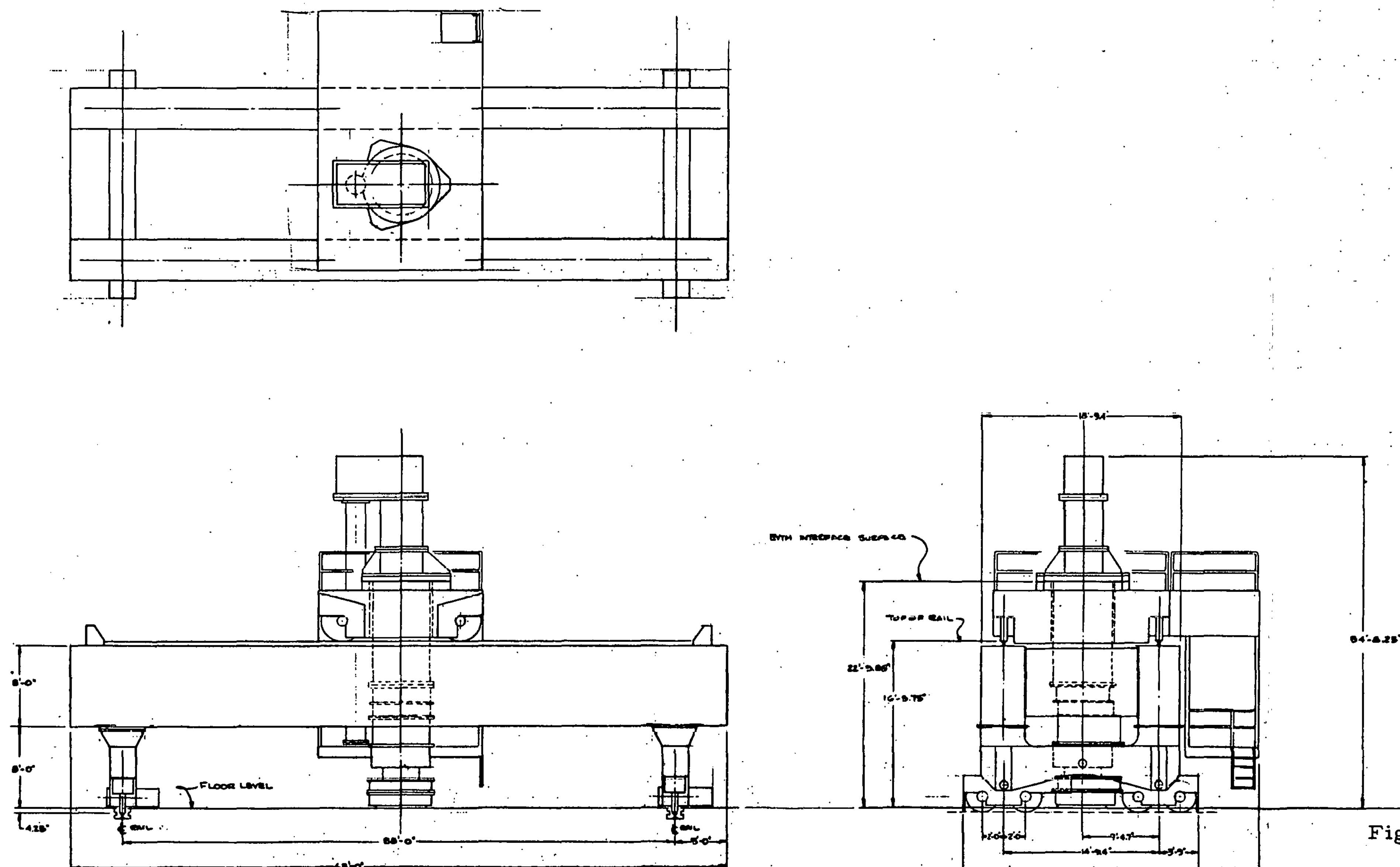

Figure 30. CRBRP Conceptual EVTM Gantry (Drawing No. N099413014)

The EVTM weight savings of 86,000 lb should result in an estimated fabrication cost savings of $428,000. The gantry size reduction fabrication cost savings is estimated at $50,000 for a total savings of $478,000.

The shortened EVTM study report was combined with the Grapple-Chain Trade Study Report (TSR-099-413-001).

c. Core Component Pot (CCP) Syphon Study

Thermal analysis determined that a fuel element generating 20 kwt will cause the sodium in the CCP to reach an equilibrium average temperature of 1000°F within the EVTM. If the CCP temperature starts at a reactor sodium pool temperature of 450°F, the sodium volume within the CCP will expand by ~10%. The estimated 4-mil coating on the grapple will cause additional sodium to drain into the CCP.

In order to minimize the number of times a drip pan must be changed during refueling, a CCP concept, using a syphon to lower the sodium level within the fuel element as it is removed from the reactor, has been developed. This provides containment for the expansion, eliminating or reducing sodium overflow into the drip pans. It should also improve emissivity for heat transfer by reducing the time the CCP is coated with a sodium film. An overall CCP length of 8.5 in. greater than the reference design is required to prevent all overflow from the pot. Analysis of the concept is underway and is being pursued concurrently with syphon test planning.